Electronic Supplementary Information

Intense chirality induction in nitrile solvents by a helquat dye monitored by near resonance Raman scattering

Jaroslav Šebestík,*[a] Filip Teplý,*[a] Ivana Císařová,[b] Jan Vávra,[a] Dušan Koval[a] and Petr Bouř*[a]

[a] Institute of Organic Chemistry and Biochemistry, Academy of Sciences of the Czech Republic, v.v.i., Flemingovo n. 2, 166 10 Prague 6, Czech Republic. E-mail: sebestik@uochb.cas.cz, teply@uochb.cas.cz, bour@uochb.cas.cz

[b] Department of Inorganic Chemistry, Charles University, Hlavova 2030/8, 128 43 Prague 2, Czech Republic

Table of contents

Fig. S1 Raman spectra of [6]helquat dye (HQ) in three nitrile solvents.

Fig. S2 Raman spectra of HQ – details.

Fig. S3 Raw ROA and Raman spectra of HQ in HCN.

Fig. S4 Raw ROA and Raman spectra of HQ in ACN.

Fig. S5 Raw ROA and Raman spectra of HQ in ACN-*d3*.

Fig. S6 Comparison of raw Raman spectra of HQ in five different solvents.

Fig. S7 Simulated Raman and ROA spectra of HQ.

Fig. S8 The transition polarizability model.

Fig. S9 Raman and ROA spectra of HQ in ACN/propionitrile mixtures.

Fig. S10 Examples of molecular orbitals of a complex of ACN and HQ.

Fig. S11 Chiral analysis of helquat dye precursor using capillary electrophoresis.

Fig. S12 Chiral analysis of helquat dye (HQ) using capillary electrophoresis.

Table S1 Frequencies of the CN stretching vibration in different solvent systems.

Table S2 Energies and populations of two HQ conformers.

Table S3 Influence of HQ on enhancement of ACN vibrations in ten randomly selected clusters from first solvation sphere.

Experimental and Computational Details

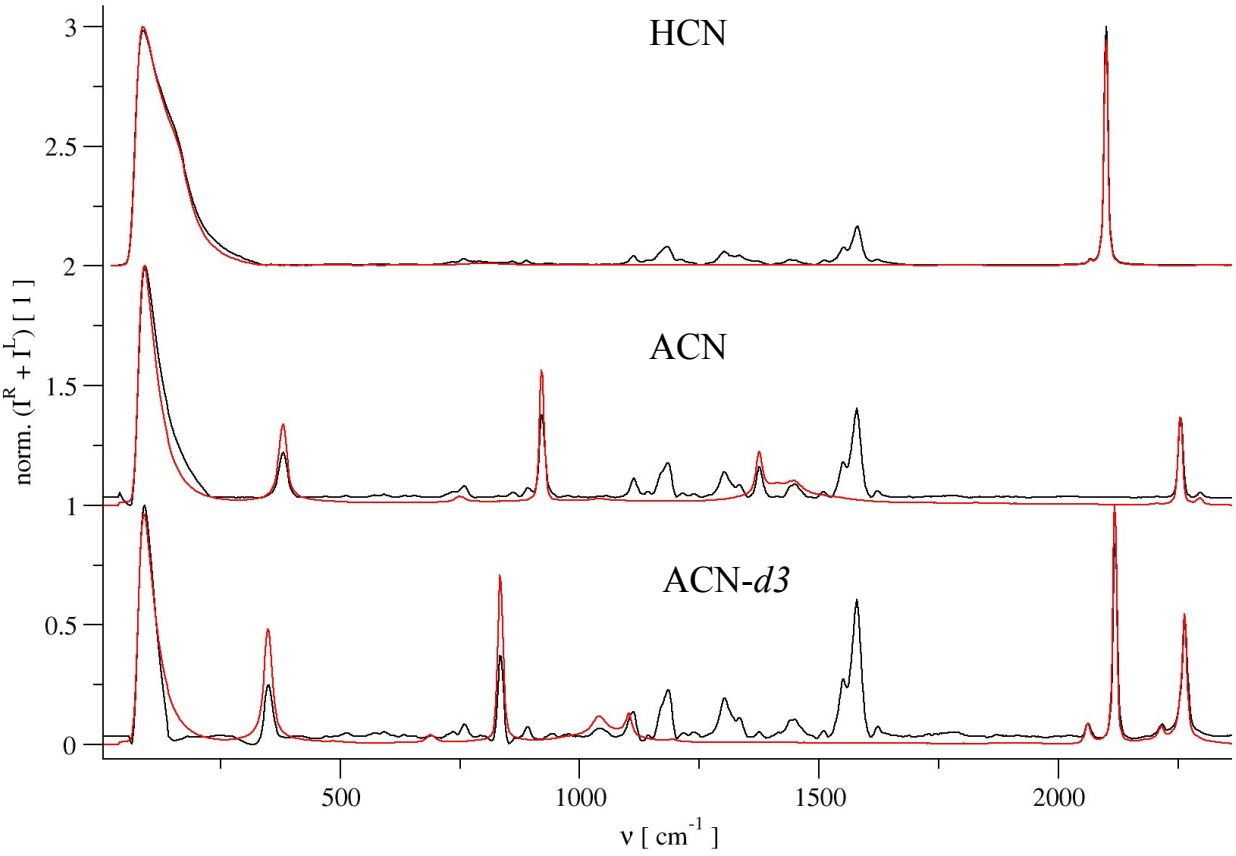

Fig. S1 Experimental resonance Raman spectra of HQ in HCN, ACN, and ACN-d_3 solvents for concentration ~ 9 x 10^{-5} M (curves plotted in black). Curves plotted in red correspond to the neat solvent spectra. ACN = acetonitrile.

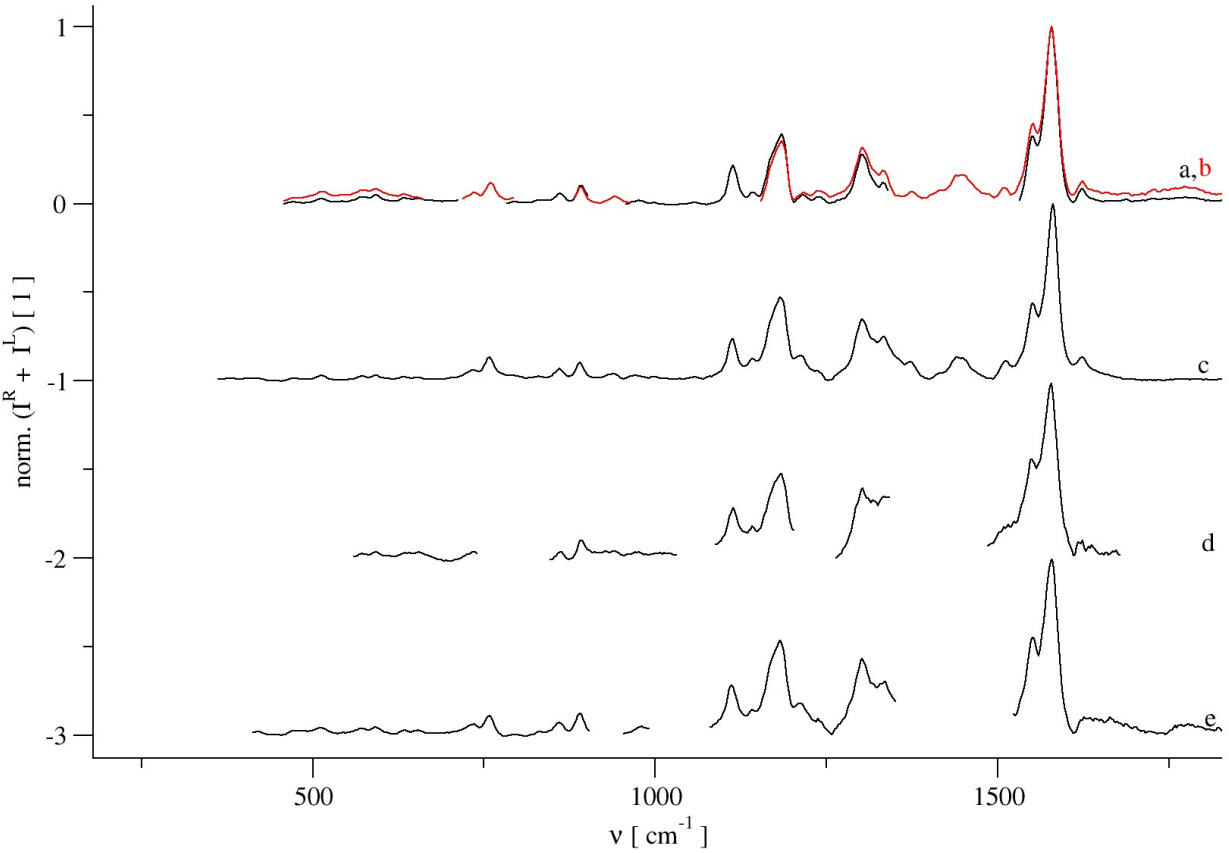

Fig. S2 Experimental Raman spectra of HQ a) in ACN, b) in ACN-*d3*, c) in HCN, d) in acetone, and e) in MeOH/ACN 7:1 mixture. Regions affected by the solvents were deleted.

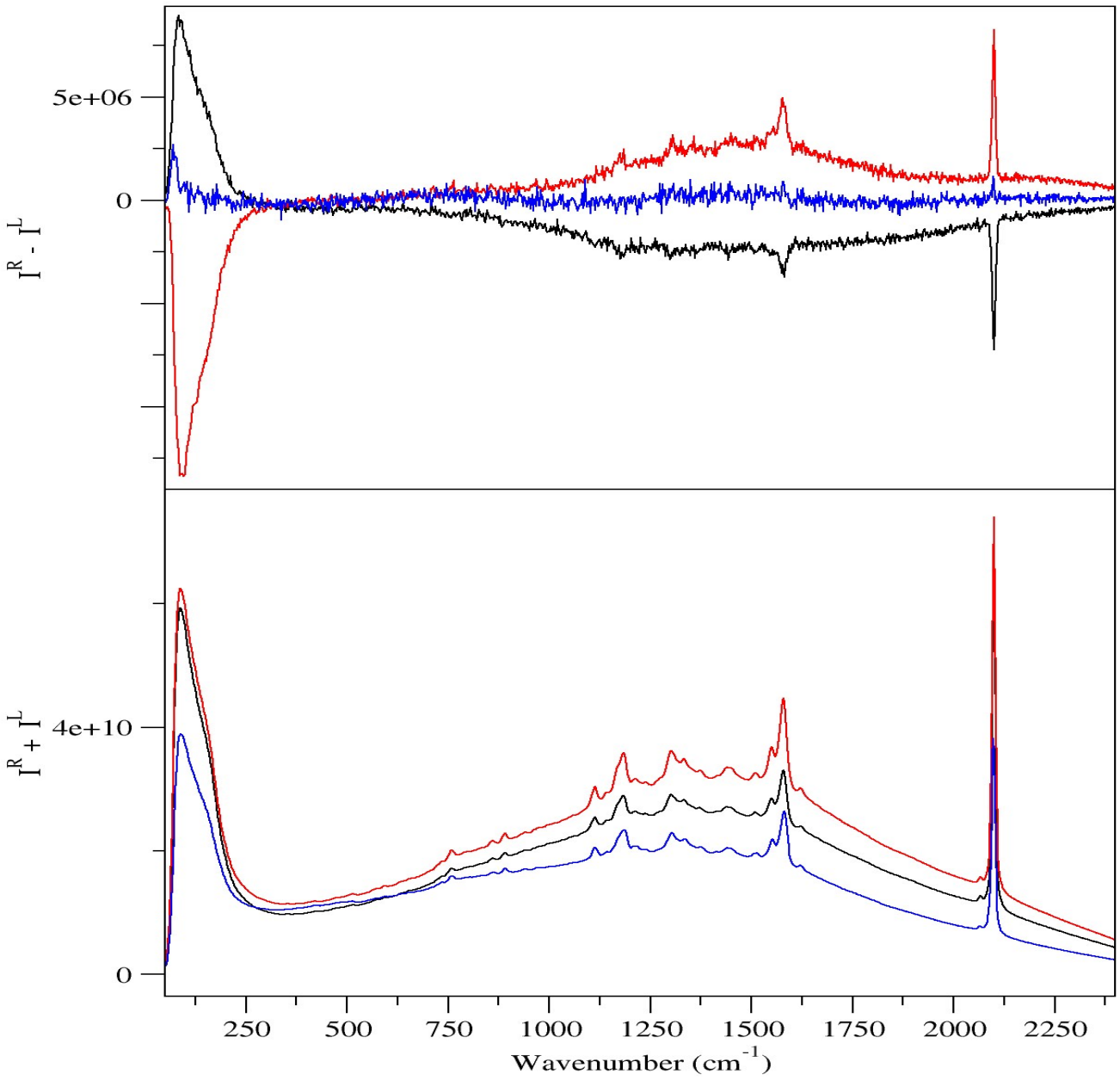

Fig. S3 Raw experimental ROA ($I^R - I^L$) and Raman ($I^R + I^L$) spectra of HQ in liquid HCN at 10 °C. The black and red colors correspond to *P* and *M* enantiomers, respectively. Blue stands for the racemate.

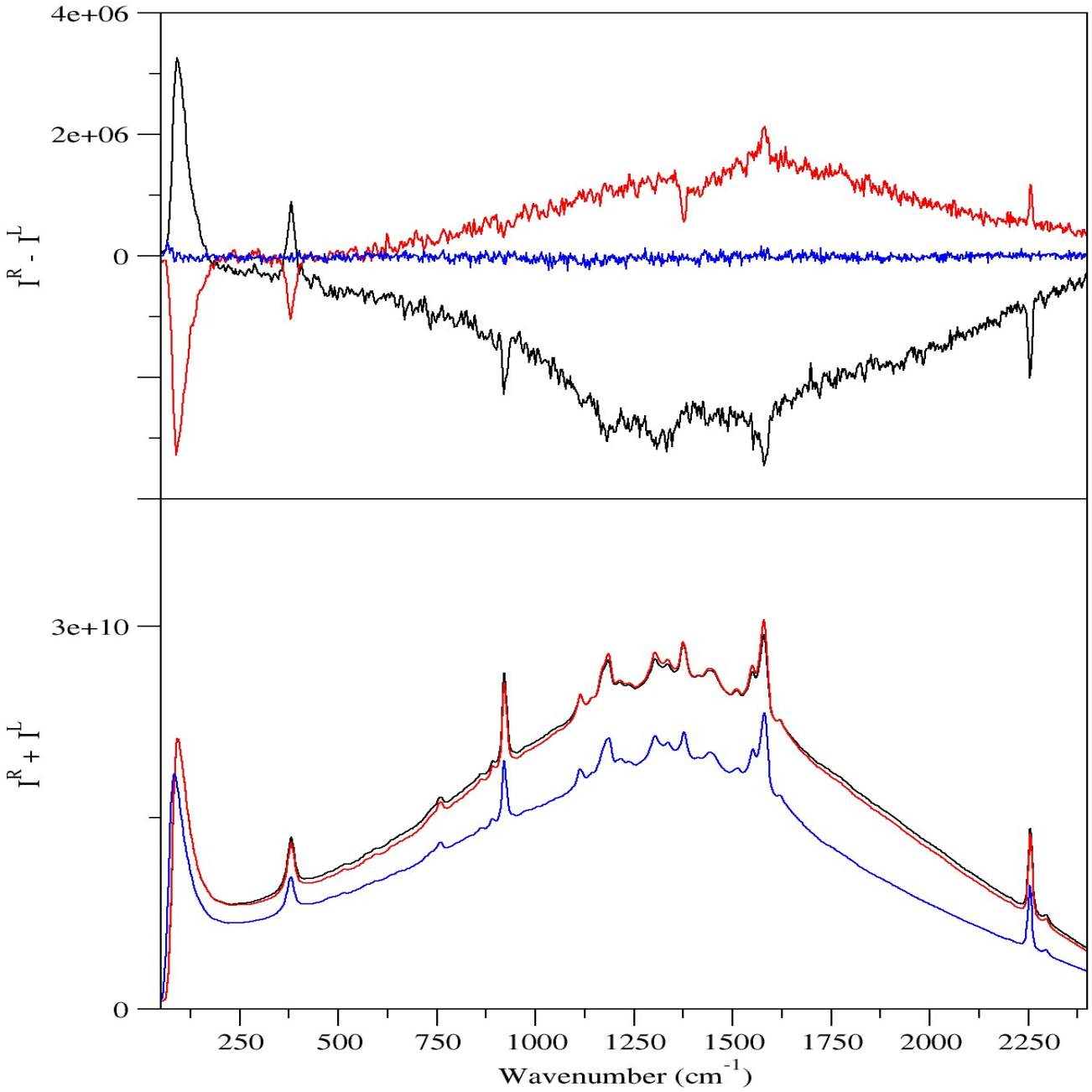

Fig. S4 Raw ROA and Raman spectra of HQ in ACN measured at room temperature (ca 21-23 °C). The black and red curves correspond to *P* and *M* enantiomers, respectively. Blue color stands for the racemate.

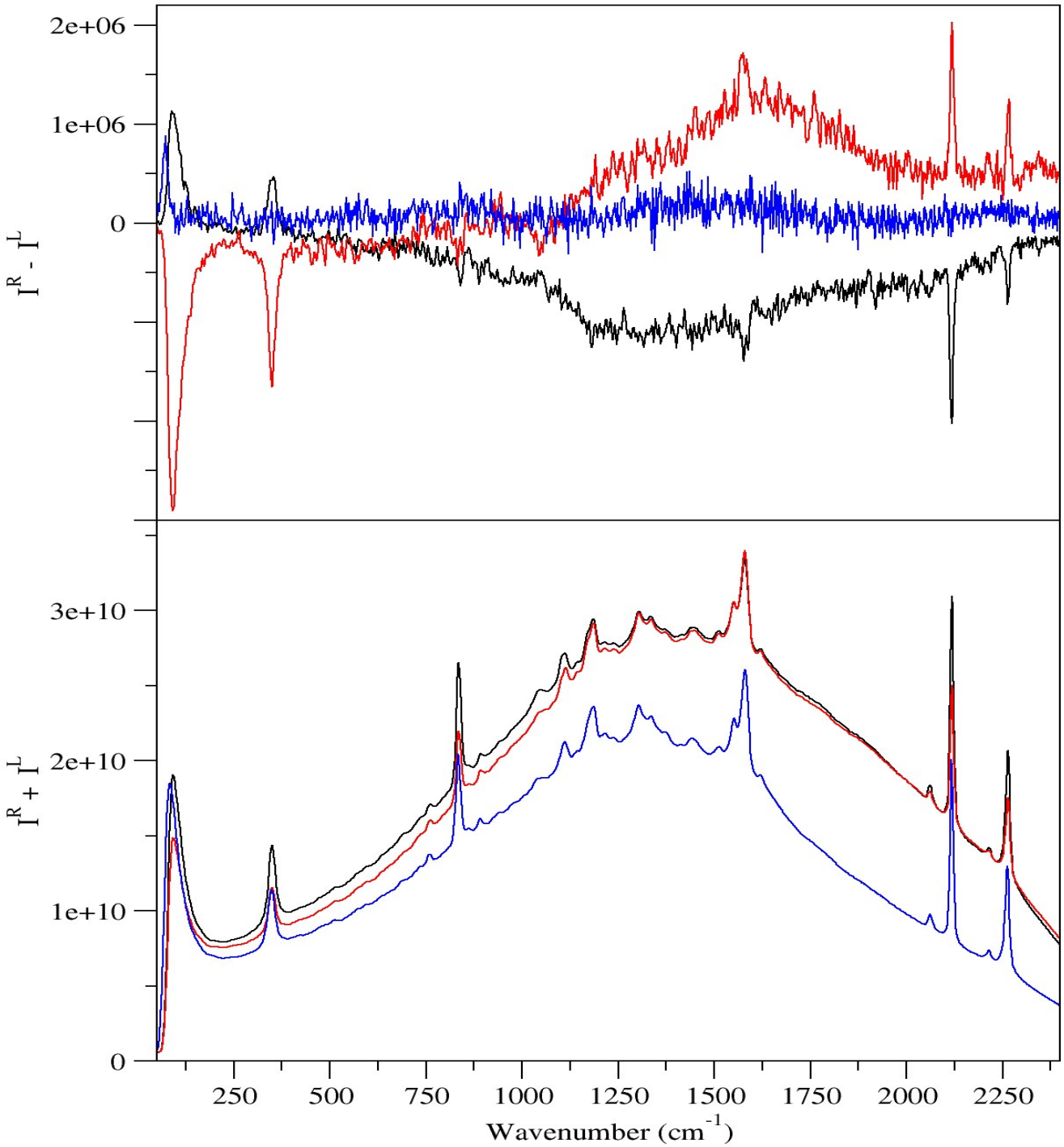

Fig. S5 Raw ROA and Raman spectra of HQ in ACN-d_3 at 21 °C. The black and red curves correspond to *P* and *M* enantiomers, respectively. Blue color stands for the racemate.

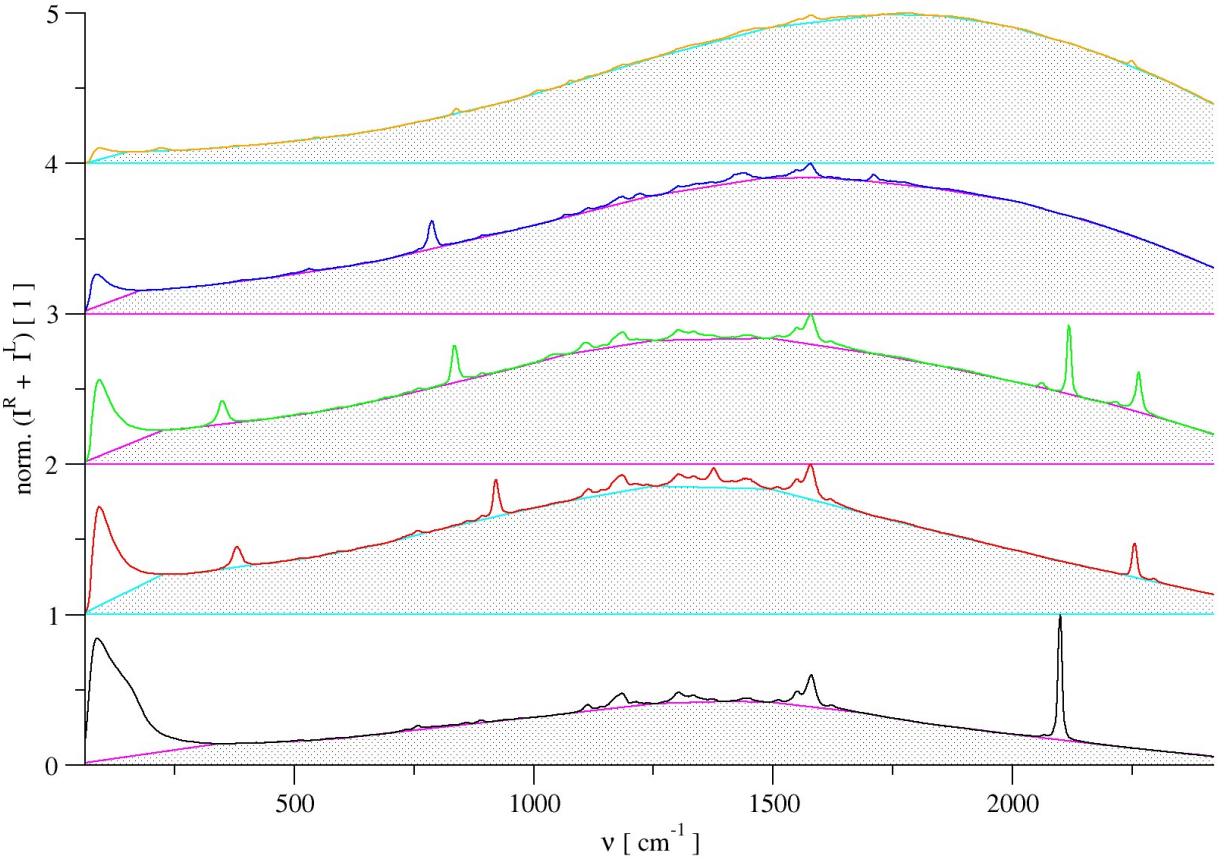

Fig. S6 Raw Raman spectra of HQ in HCN (black curve), ACN (red), ACN-d_3 (green), acetone (blue), and propionitrile (orange), from bottom to top, ordered by increasing fluorescence emphasized by the grey areas.

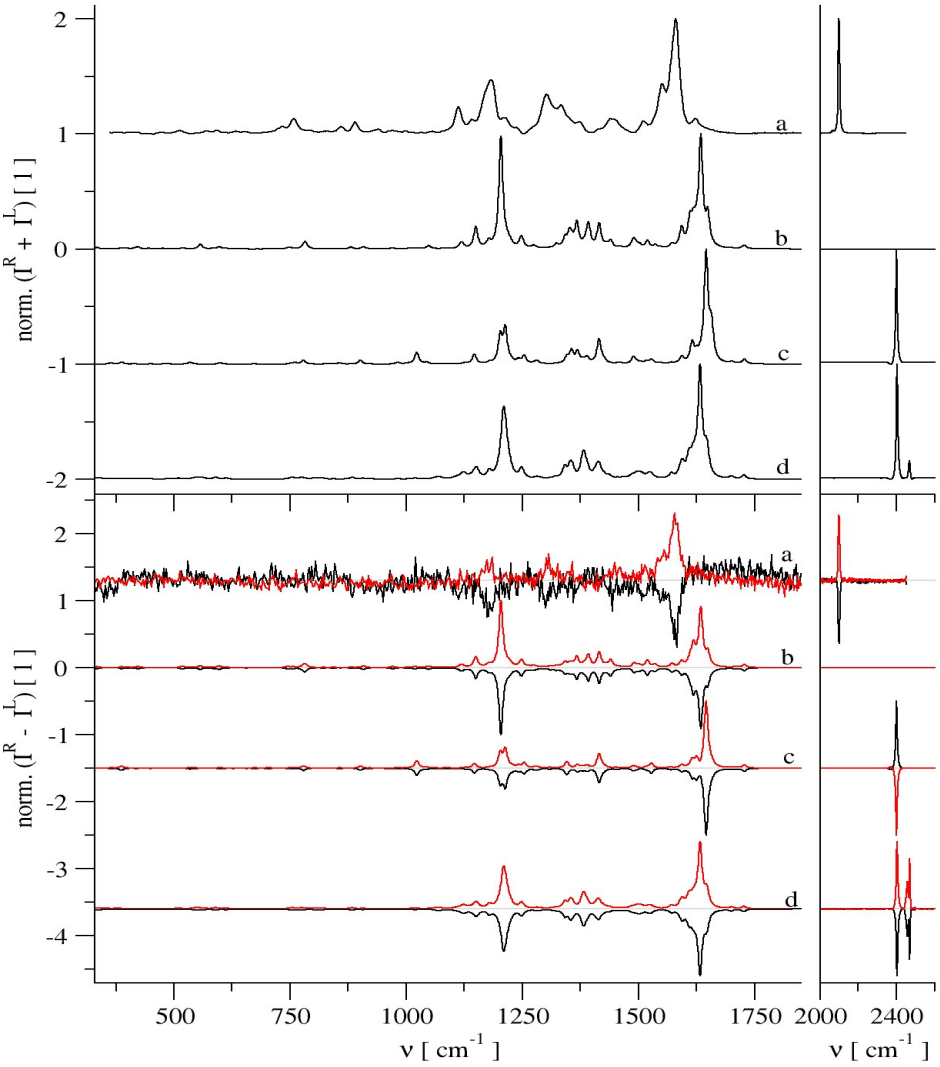

Fig. S7 Raman and ROA spectra of HQ. (a) Experiment in HCN, and (b-d) CAM-B3LYPD/6-31+G**/CPCM calculations: (b) HQ only, (c) HQ/ACN (one molecule) complex and (d) averaged spectrum obtained from 58 HQ/ACN MD clusters. The black and red curves in ROA spectra correspond to *P* and *M* enantiomers, respectively; the CN regions in (c) and (d) were multiplied by 1500 and 280000. Due to very low fluorescence of HQ in HCN, the experimental spectrum of HQ had higher signal to noise ratio as compared to that in ACN. Thus, the relatively less intense HQ bands from the experiment can be best compared with calculation when HCN solvent was used.

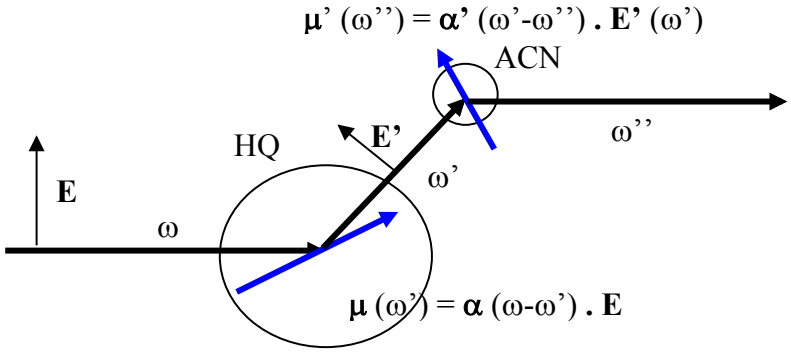

Fig. S8 The transition polarizability model (TPM). The transition polarizabilities assigned to solvent (ACN solvent) and solute (HQ) molecules allow for a change of the wavenumber of the incident radiation. For example, in the helquat (HQ) electric dipole moment (**μ**) oscillating with frequency ω’ is induced by the laser radiation of frequency ω. Its electric field (**E’**) may induce in ACN another dipole (**μ’**) with the same or different frequency. For ROA, the magnetic and quadrupole polarizabilities are included as well.

Table S1 Experimental frequencies of CN stretching vibration in different solvent systems.

Solvent with helquat	ν_{CN} cm^{-1}	$\Delta\nu_{CN}$ cm^{-1}	**ROA of CN**
HCN	2099	0	yes
CH_3CN	2256	2	yes
CD_3CN	2265	2	yes
CH_3CH_2CN	2249	0	fluorescence
CH_3CN/CCl_4 1:7	2256	0	fluorescence
CH_3CN/CH_3COCH_3 1:7	2254	0	no
CH_3CN/CH_3OH 1:7	2258	0	no
CH_3CN/CCl_4 7:1	2254	0	yes
CH_3CN/CH_3COCH_3 7:1	2254	0	yes

ν_{CN} vibration of nitrile group in helquat solution
$\Delta\nu_{CN} = \nu_{CN} - \nu_{CN}$(without helquat)

Table S2 HQ energies and conformer populations predicted at various levels of theory.

Isomer	ΔE [kcal.mol^{-1}]	Distribution [%]	Method
A	0.49	31	B3LYP/6-311++G**/CPCM,ACN
B	0.00	69	B3LYP/6-311++G**/CPCM,ACN
A	0.46	31	B3LYP/6-31+G**/CPCM,ACN
B	0.00	69	B3LYP/6-31+G**/CPCM,ACN
A	0.45	32	B3LYP/6-31+G**/CPCM,H_2O
B	0.00	68	B3LYP/6-31+G**/CPCM,H_2O
A	0.00	78	B3LYPD/6-31+G**/CPCM,ACN
B	0.76	22	B3LYPD/6-31+G**/CPCM,ACN
A	0.00	93	CAM-B3LYPD/6-31+G**/CPCM,ACN
B	1.52	7	CAM-B3LYPD/6-31+G**/CPCM,ACN

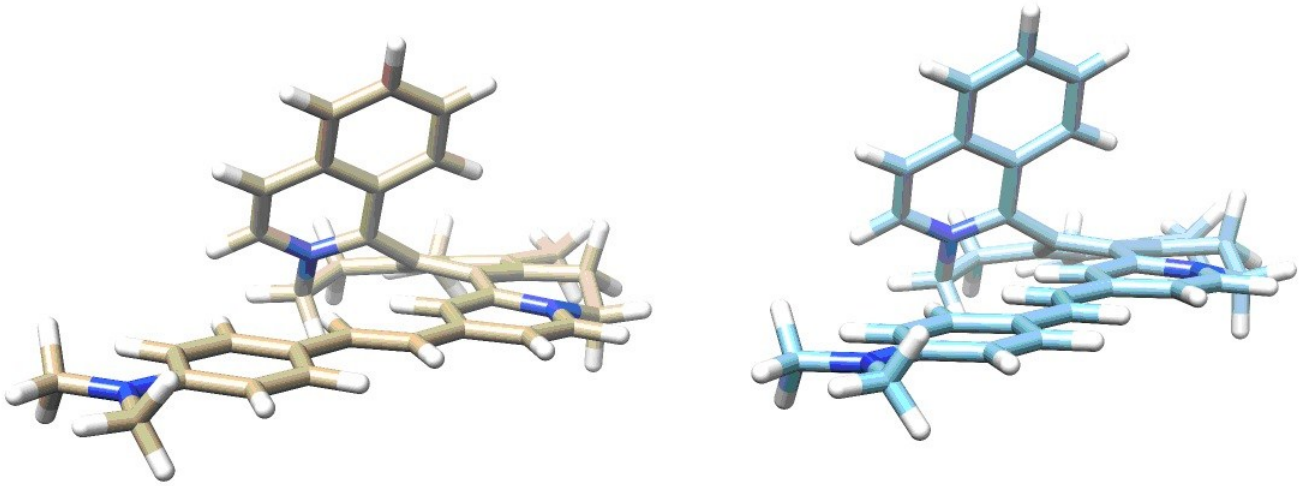

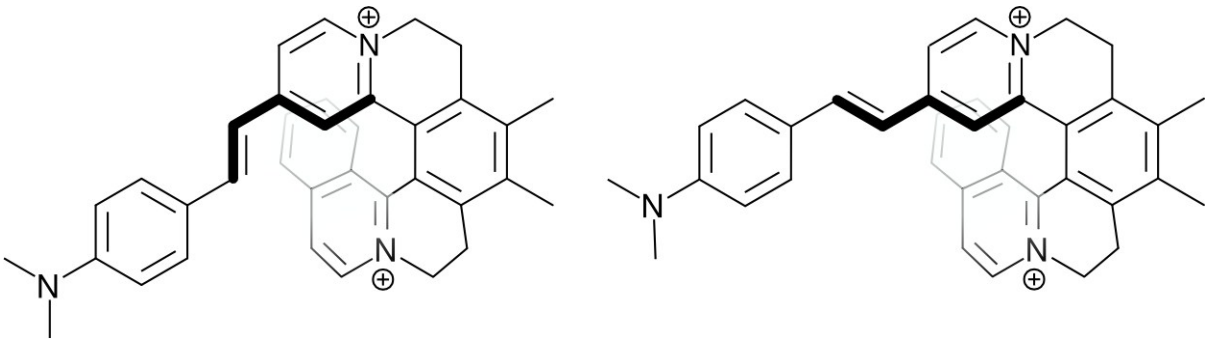

s-cis conformer of (*P*)-helquat

s-trans conformer of (*P*)-helquat

Table S3 Influence of HQ on enhancement of ACN vibrations in ten randomly selected clusters from the first solvation sphere of $HQ(ACN)_{34\text{-}41}(Cl^-)_{0\text{-}1}$. Two most intense vibrations (I and II) are listed. Cluster **j** corresponds to that from Fig. 3 in the manuscript. Sometimes individual ROA intensities are very intense; however, the opposite signs of other oscillator can lead almost to the cancellation of overall ROA signal. *E.g.* in cluster **i**, the most intense vibration is ca 25 times more intense than overall ROA spectrum. Cluster properties were calculated at BPW91/STO-3G level.

Cluster	ROA intensity $_{CN\ cluster}$ [a.u.][a)]	Enhancement (I) [%][b)]	Enhancement (II) [%][b)]
a	-138	160	-34
b	-1.3	-355	158
c	-690	35	11
d	-124	42	16
e	57654	28	24
f	-722	64	25
g	-13	149	-45
h	-13	117	-17
i	-0.05	2520	1940
j	6×10^6	32	18

[a)] Sum of intensities of all nitrile vibrations contributing to the total simulated intensity of CN signal associated with the individual clusters.

[b)] 100% intensity corresponds to the ROA intensity of all CN vibrations in the cluster.

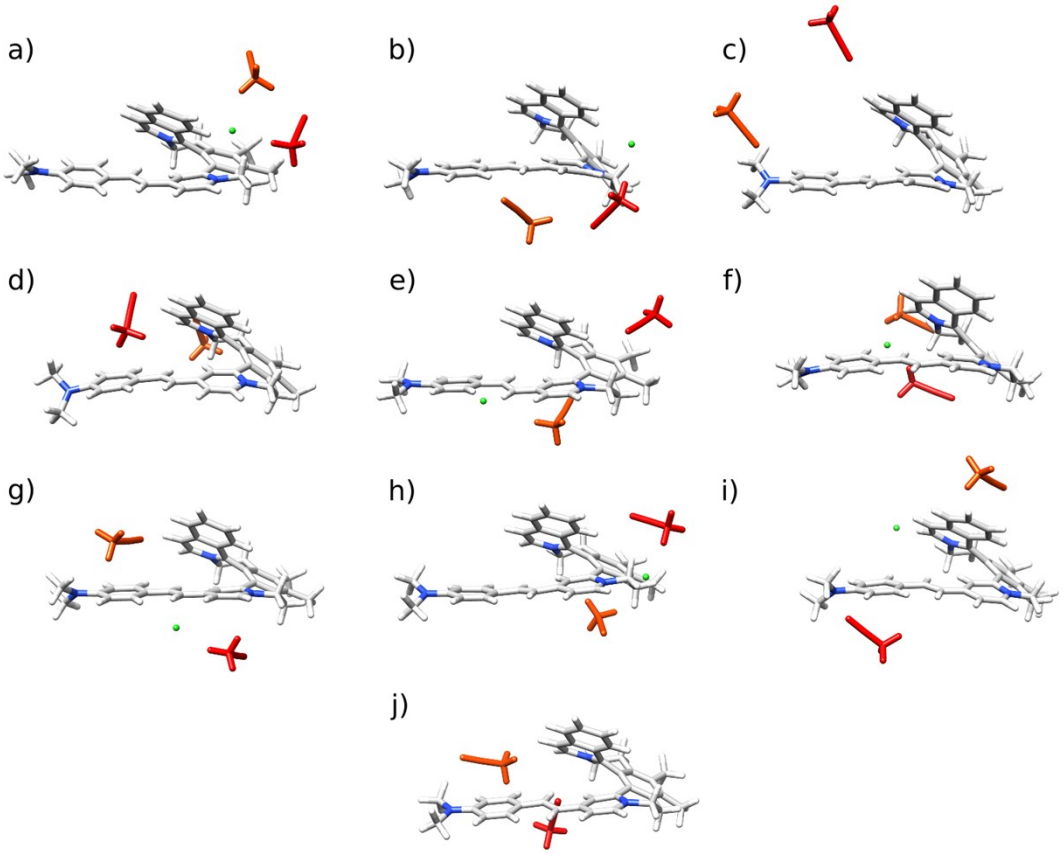

Raman spectra and ROA spectra in solvent mixtures

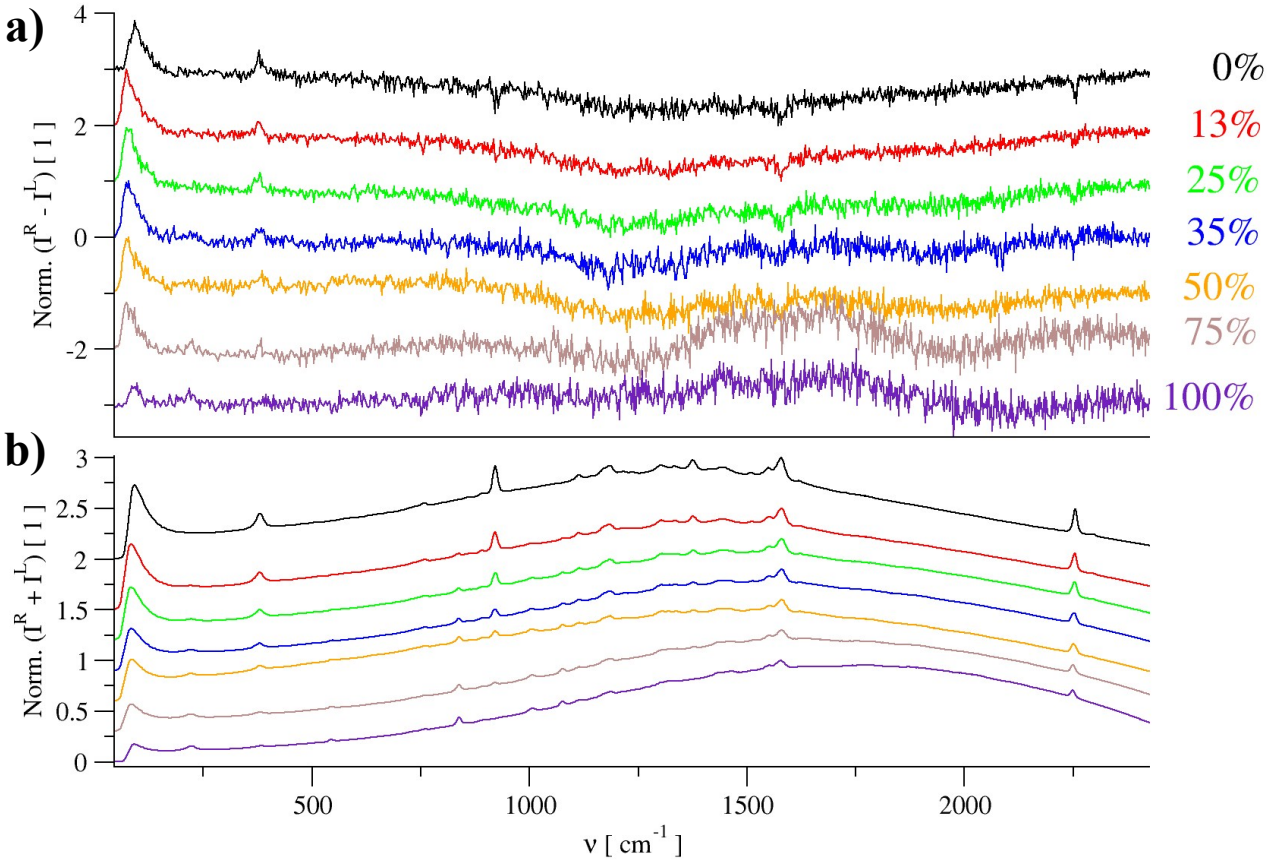

Fig. S9 Raman (b) and ROA (a) spectra of HQ (0.07 mg/mL) in ACN/propionitrile mixtures. Propionitrile percentage is indicated. Propionitrile co-solvent is accompanied by a strong fluorescence and Raman signal becomes relatively weak (cf. also Fig. S6). Solvatochromic fluorescence shift can be observed in b. At 25% of propionitrile, induced ROA is still apparent, whereas at 35% it vanishes.

ROA spectra in methanol/ACN mixtures

For HQ solution (0.07 mg/mL) in 1:7 methanol:ACN mixture the induced ROA drops down to about half as compared to a solution of HQ in neat ACN. ROA vanishes at 26% methanol in ACN.

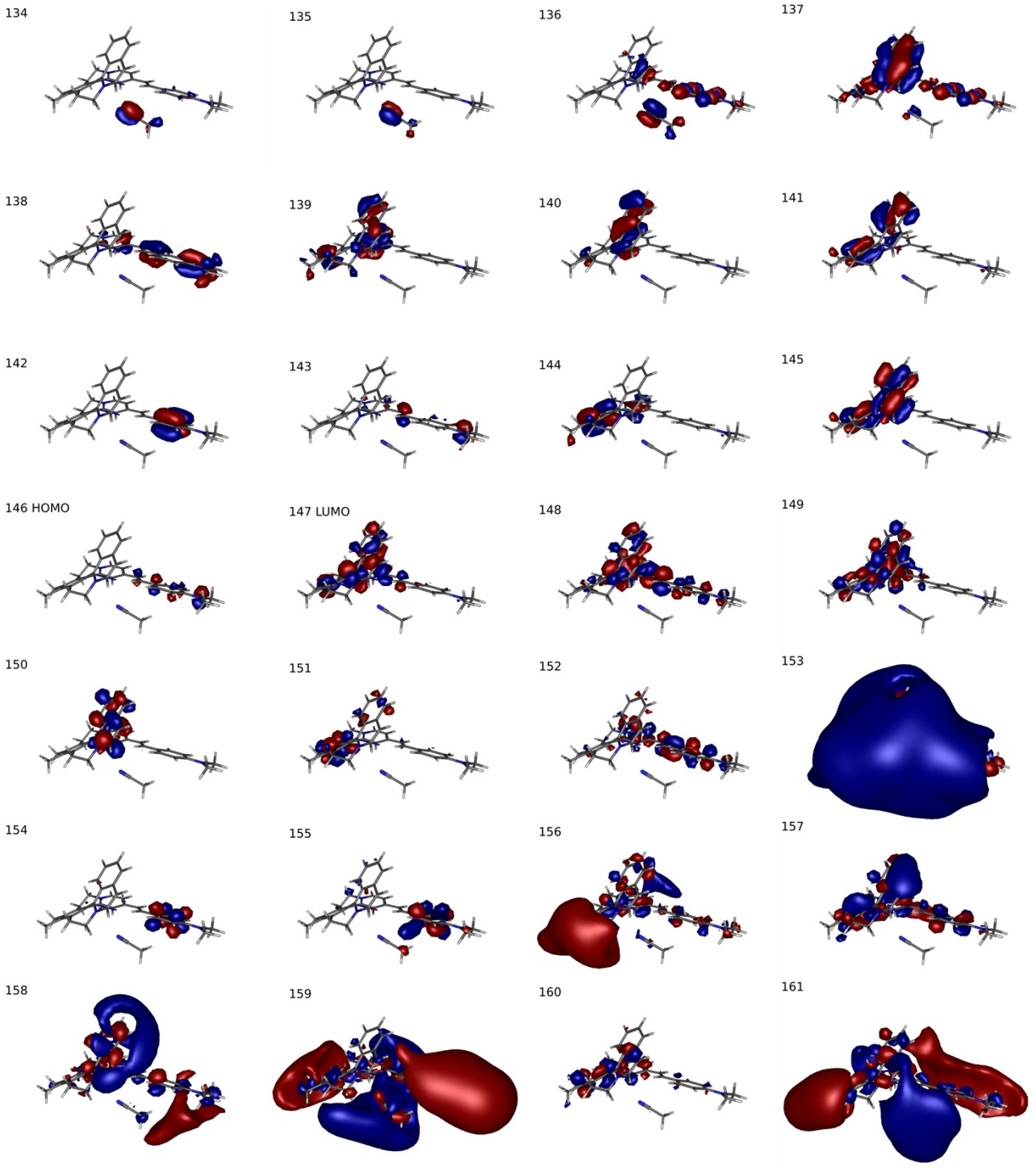

Fig. S10 Examples of molecular orbitals of a complex of ACN and HQ exhibiting enhanced Raman intensity of the CN solvent stretching band (HOMO/LUMO orbitals are 146/147).

Experimental and Computational Details

Spectra Measurement

Raman and ROA spectra were obtained using a ChiralRAMAN-2X instrument operating with 532 nm laser light, 7 cm^{-1} resolution, and SCP (scattered circular polarized) back-scattering configuration. Laser power at the sample was 59 mW. Illumination time was 12-24 hours for each enantiomer (corresponding to acquisition time of 24-48 hours). Illumination times 24 hours were used only for measurement of (*M*)-enantiomer in ACN and ACN-*d3*. For propionitrile titration experiments, acquisition times were ca 6 hours. For the measurement with liquid HCN, home-made temperature cell was used, which maintained the HCN temperature at 10 ^{o}C i.e. ca 16 $^{\circ}$C below its boiling point. The windows of cell were exposed to flowing dry N_2 in order to prevent water condensation. The spectra were processed by home-made software published earlier.[1]

The detection limit of resonance Raman is 5×10^{-7} M of HQ in nitrile solvent. However, the detection limit for enhanced ROA of CN group is 3×10^{-5} M of HQ in nitrile solvent (0.02 mg/mL), where the absorption of HQ at 532 nm is 0.5. This concentration corresponds to HQ:solvent ratios of ca 1:1,000,000 for HCN, 1:700,000 for ACN, and 1:700,000 for ACN-*d3*. Optimal concentration of HQ to study the phenomenon throughout this report is 0.07 mg/mL ($c_{HQ} = 9\times10^{-5}$ M), *i.e.* HQ:solvent ratios 1:200,000 for ACN.

Computations

MD simulation of solvated helquat was carried out using Amber 10,[2] Packmol,[3] and Chimera[4] software packages. The helquat was immersed into a cubic box ($40\times40\times40$ Å^3) containing 738 ACN molecules and 2 chloride anions. The geometry was minimized and equilibrated with free dynamics within 5 ns at 300 K . Resultant trajectory was analyzed by programs ptraj (Amber 10 suit) and Chimera.

Clusters with ACN distance of 3.5 Å from helquat were selected and 58 of them were used for generation of the spectra using the Cartesian coordinate tensor transfer method (CCT)[5] and the CAM-B3LYPD/6-31+G**/CPCM=Acetonitrile level[6] for individual molecules.

Alternatively, the BPW91/STO-3G level was used for ad hoc selected cluster of $HQ(ACN)_{34-41}(Cl^-)_{0-1}$.[7]

The transition polarizability model[8] was used to generate ROA and Raman spectra of HQ/ACN clusters as well. In this model the helquat and solvent molecules were replaced by electric dipole-electric dipole ($\boldsymbol{\mu}$), magnetic dipole-electric dipole (**G'**) and electric quadrupole-electric dipole (**A**) transition polarizabilities, obtained from the polarizability derivatives and force field (FF). The polarizability derivatives and FF were calculated by Gaussian at the #B3LYP/6-31+G** SCRF(CPCM,Solvent=Acetonitrile) level. Then the transition polarizabilities were transferred to the solvent and solute molecules in snapshot geometries obtained during the MD run and resultant polarizabilities and Raman and ROA spectra calculated. By this procedure a large number of MD geometries can be averaged.

Organic Synthesis, General

Thin-layer chromatography (TLC) analysis of the organic cations was performed using silica gel plates (Silica gel 60 F_{254}-coated aluminium sheets, Merck, cat. no. 1.05554.0001) with Stoddart's magic mixture (MeOH:NH_4Cl aq (2M):$MeNO_2$ 7:2:1) used as an ionic mobile phase.[9] Visualization of compounds after separation on TLC plates was performed by UV (UV lamp 254/365 nm, Spectroline® Model ENF – 240C/FE). Melting points were determined on a Wagner & Munz PolyTherm A micro melting point apparatus and are uncorrected. If necessary, DMSO was removed from NMR samples using a Labconco evaporator (Refrigerated CentriVap Benchtop Vacuum Concentrator, cat. no. 7310031). Sonication was conducted with a Bandelin Sonorex sonicator. NMR spectra were measured on a Bruker Avance 600 (600 MHz for ^{1}H, 151 MHz for ^{13}C) NMR spectrometer. In ^{1}H and ^{13}C NMR spectra, chemical shifts are referenced as follows (ppm): in acetone-*d*6 the peaks were referenced relative to the solvent peak δ_H = 2.09 ppm and δ_C = 29.80 ppm; in DMSO-*d*6 δ_H = 2.50 ppm and δ_C = 39.50 ppm. Chemical shifts are given in δ-scale as parts per million (ppm); coupling constants (*J*) are given in Hertz. IR spectra were recorded on a Bruker Equinox 55 (IFS55) spectrometer. Abbreviations for intensities of IR bands are as follows: s for strong, vs for very strong, m for medium, w for weak, vw for very weak, br for broad, sh for shoulder. Mass spectral data were obtained at the Mass Spectrometry Facility operated by the Institute of Organic Chemistry and Biochemistry, Academy of Sciences of the Czech Republic, v.v.i. (IOCB ASCR). ESI mass spectra were recorded using a Thermo Scientific LCQ Fleet mass spectrometer equipped with an electrospray ion source and controlled by Xcalibur software. The mobile phase consisted of methanol : water (9:1), flow rate of 200 μL.min^{-1}. The sample was dissolved, diluted with the mobile phase and injected using a 5 μL loop. Spray voltage, capillary voltage, tube lens voltage and capillary temperature were 5.5 kV, 5 V, 80 V and 275 °C, respectively. HR MS spectra were obtained with the ESI instrument. Specific rotation values were determined with an Autopol IV (Rudolph Research Analytical, USA, 2001) polarimeter. Specific rotation $[\alpha]_D^{20}$ was measured in concentration *c* (g/100 mL) and solvent as specified in each case. Demineralized water obtained from the Water Purification Facility at the IOCB ASCR was used unless otherwise stated. Demineralization was accomplished by way of filtration through ion exchange columns (Lewatit S100 for catex column, Lewatit MP500 for anex column) in a demineralization ion exchange station type ID-PP and IDKP (Kavalier, Votice, Czech Republic). DMSO-d_6 was dried over 4 Å molecular sieves. Enantiocomposition analysis was performed using capillary electrophoresis (CE) with cyclodextrin-based chiral selector as detailed in the section on Chiral analysis. Unless otherwise stated, all starting materials and reagents were obtained from commercial suppliers and used without further purification. Racemic sample [*rac*-**1**][TfO]$_2$ was obtained according to literature procedure.[10] Ion exchanges using ion exchange resin were performed using strongly basic anion exchange resin Dowex 1 x 2; 16-100, Cl^- cycle (Supelco, 13367) according to procedures detailed in reference 11.

Synthetic Procedures and Analytical Data

Mixture of diastereoisomeric salts [*P*-1][(*R*,*R*)-dibenzoyltartrate]$_2$ and [*M*-1][(*R*,*R*)-dibenzoyltartrate]$_2$

(*P*)-6,7,13-Trimethyl-4,5,8,9-tetrahydroisoquinolino[1,2-a]pyrido[1,2-k][2,9]phenanthroline-3,10-diium (2*R*,3*R*)-2,3-bis(benzoyloxy)-3-carboxypropanoate and
(*M*)-6,7,13-Trimethyl-4,5,8,9-tetrahydroisoquinolino[1,2-a]pyrido[1,2-k][2,9]phenanthroline-3,10-diium (2*R*,3*R*)-2,3-bis(benzoyloxy)-3-carboxypropanoate

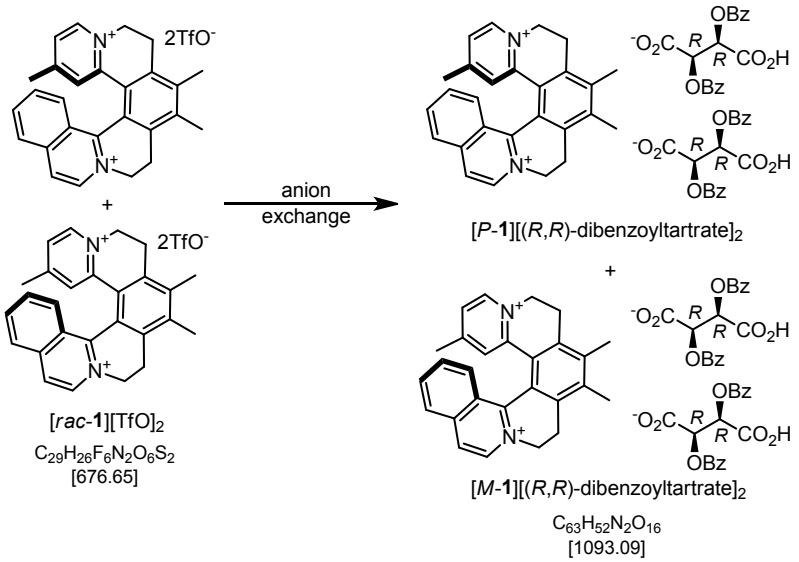

[*rac*-**1**][TfO]$_2$ (651 mg, 0.962 mmol) was dissolved in MeOH (10 mL) and transferred onto an ion exchange resin loaded with (*R*,*R*)-dibenzoyltartrate anions (bed volume of the resin in the column was *ca* 40 mL; for loading procedure, see ref. 11). The solution of helquat was allowed to slowly sink into the ion exchange resin (flow rate approximately 2 drops per second). Then, MeOH (200 mL) was passed through the resin to elute the helquat (flow rate *ca* 2 drops per second; TLC detection of helquat in the eluent). The volatiles from the eluted solution obtained were removed on rotary evaporator giving a light brown solid (972 mg, $[\alpha]_D$ = -55.2, c = 0.328, MeOH).

[*M*-1][(*R*,*R*)-dibenzoyltartrate]$_2$

(*M*)-6,7,13-Trimethyl-4,5,8,9-tetrahydroisoquinolino[1,2-a]pyrido[1,2-k][2,9]phenanthroline-3,10-diium (2*R*,3*R*)-2,3-bis(benzoyloxy)-3-carboxypropanoate

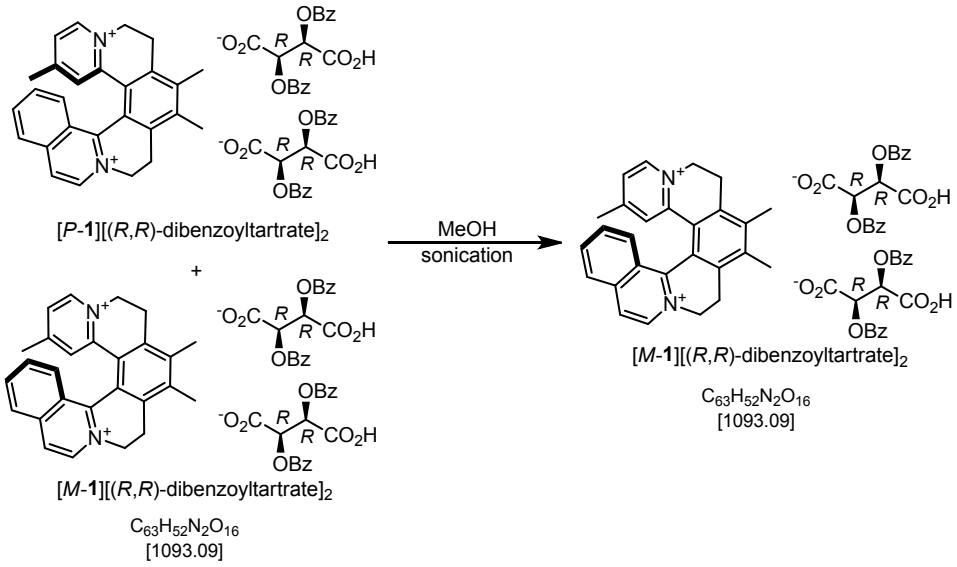

Mixture of diastereoisomeric salts [*P*-**1**][(*R*,*R*)-dibenzoyltartrate]$_2$ and [*M*-**1**][(*R*,*R*)-dibenzoyltartrate]$_2$ (972 mg) was suspended in MeOH (3 mL) and sonicated for 5 min. The resulting suspension was centrifuged and the supernatant was separated giving 633 mg of a solid which was a diastereomerically enriched mixture of salts ($[\alpha]_D$ = -231.7, c = 0.293, MeOH, 39 % *de* according to CE). The procedure of sonication, centrifugation and supernatant removal was repeated 5 more times giving 421 mg of the [*M*-**1**][(*R*,*R*)-dibenzoyltartrate]$_2$ as an off-white solid (0.385 mmol, 87 % yield of (*M*,*R*,*R*)-diastereomer; $[\alpha]_D$ = -465.6, c = 0.233, MeOH; 97 % *de* according to CE). **Mp**: 155-157 °C; **^{1}H NMR** (600 MHz, DMSO-d_6): δ = 1.86 (s, 3H), 2.48 (s, 6H), 3.04-3.12 (m, 1H), 3.16-3.24 (m, 1H), 3.51-3.60 (m, 2H), 4.80 (dt, *J* = 3.7, 14.4 Hz, 1H), 5.01-5.09 (m, 2H), 5.16-5.21 (m, 1H), 5.60 (s, 4H), 7.20 (bd, *J* = 1.9 Hz, 1H), 7.42-7.47 (m, 8H), 7.54-7.61 (m, 6H), 7.82 (dd, *J* = 8.7, 0.8 Hz, 1H), 7.86-7.90 (m, 8H), 7.90-7.93 (m, 1H), 8.18 (d, *J* = 8.2 Hz, 1H), 8.51 (d, *J* = 6.6 Hz, 1H), 8.94 (d, *J* = 6.3 Hz, 1H), 9.05 (d, *J* = 6.7 Hz, 1H); **^{13}C NMR** (151 MHz, DMSO-d_6): δ = 16.5, 16.6, 20.4, 24.8, 25.2, 53.1, 54.4, 71.2, 122.2, 124.2, 125.2, 125.8, 126.5, 127.7, 128.6, 129.1, 129.3, 129.6, 131.2, 133.3, 134.9, 2 x 136.6, 137.6, 138.1, 139.5, 140.7, 141.0, 144.4, 145.3, 149.7, 157.2, 164.8, 167.6; **IR** (KBr): $\tilde{\nu}$ (cm^{-1}) 3061w, 3011vw, 1716vs, 1602m, 1581w, 1551w, 1515w, 1506w, 1492vw, 1451w, 1409vw, 1376w, 1353m, 1315w, 1264vs, 1176m, 1117s, 71s, 6w; **MS** (ESI) m/z: 735 (8, $[M\text{-DBT}]^+$), 377 (100, $[M\text{-2DBT-H}]^+$); **HRMS** (ESI) m/z: [M-DBT] ($C_{45}H_{39}O_8N_2$) calc. 735.27009, found 735.27033.

[*M*-1][TfO]$_2$

(*M*)-6,7,13-Trimethyl-4,5,8,9-tetrahydroisoquinolino[1,2-a]pyrido[1,2-k][2,9]phenanthroline-3,10-diium trifluoromethanesulfonate

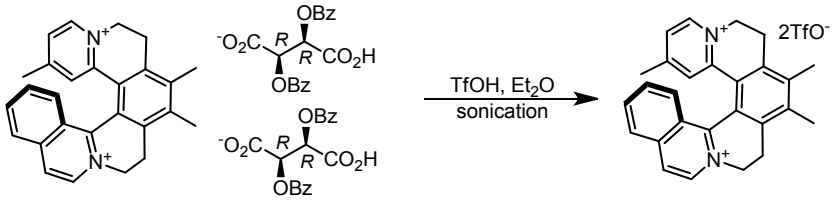

[*M*-**1**][(*R*,*R*)-dibenzoyltartrate]$_2$

$C_{63}H_{52}N_2O_{16}$
[1093.09]

[*M*-**1**][TfO]$_2$

$C_{29}H_{26}F_6N_2O_6S_2$
[676.65]

[*M*-**1**][(*R*,*R*)-dibenzoyltartrate]$_2$ (421 mg, 0.385 mmol) was suspended in triflic acid solution in Et_2O (TfOH : Et_2O = 1 : 99 volume ratio; 5 mL) and sonicated for 3 min. The resulting suspension was centrifuged and the supernatant was separated. The procedure of sonication, centrifugation and supernatant separation was repeated two more times. To remove excess of triflic acid, diethylether (5 mL) was added and the mixture was sonicated, centrifuged and the supernatant was separated. The procedure of sonication, centrifugation and supernatant separation was repeated two more times. After drying, 242 mg of [*M*-**1**][TfO]$_2$ was isolated as an off-white solid (93 %, 0.358 mmol, $[\alpha]_D$ = -633.0, c = 0.263, DMSO; 98 % *ee* according to CE). The NMR spectra were identical to those of racemic sample [*rac*-**1**][TfO]$_2$,[10] see the NMR spectra section for the NMR scan.

Mixture of diastereoisomeric salts [*P*-1][(*S*,*S*)-dibenzoyltartrate]$_2$ and [*M*-1][(*S*,*S*)-dibenzoyltartrate]$_2$

(*P*)-6,7,13-Trimethyl-4,5,8,9-tetrahydroisoquinolino[1,2-a]pyrido[1,2-k][2,9]phenanthroline-3,10-diium (2*S*,3*S*)-2,3-bis(benzoyloxy)-3-carboxypropanoate and
(*M*)-6,7,13-Trimethyl-4,5,8,9-tetrahydroisoquinolino[1,2-a]pyrido[1,2-k][2,9]phenanthroline-3,10-diium (2*S*,3*S*)-2,3-bis(benzoyloxy)-3-carboxypropanoate

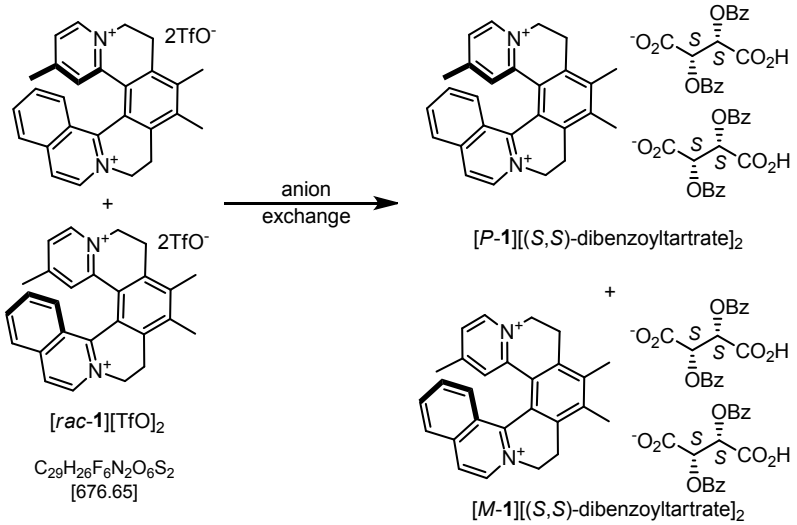

[*rac*-**1**][TfO]$_2$

$C_{29}H_{26}F_6N_2O_6S_2$
[676.65]

[*P*-**1**][(*S*,*S*)-dibenzoyltartrate]$_2$

[*M*-**1**][(*S*,*S*)-dibenzoyltartrate]$_2$

$C_{63}H_{52}N_2O_{16}$
[1093.09]

[*rac*-**1**][TfO]$_2$ (653 mg, 0.965 mmol) was dissolved in MeOH (10 mL) and transferred onto an ion exchange resin loaded with (*S*,*S*)-dibenzoyltartrate anions (bed volume of the resin in the column was *ca* 40 mL; for loading procedure, see ref. 11). The solution of helquat was allowed to slowly sink in the ion exchange resin (flow rate approximately 2 drops per second; TLC detection of helquat in the eluent). Then, MeOH (200 mL) was passed through the resin to elute the helquat (flow rate *ca* 2 drops per second). The volatiles from the eluted solution obtained were removed on rotary evaporator giving a light brown solid (923 mg, $[\alpha]_D$ = +69.6, c = 0.382, MeOH).

[*P*-1][(*S*,*S*)-dibenzoyltartrate]$_2$

(*P*)-6,7,13-Trimethyl-4,5,8,9-tetrahydroisoquinolino[1,2-a]pyrido[1,2-k][2,9]phenanthroline-3,10-diium (2*S*,3*S*)-2,3-bis(benzoyloxy)-3-carboxypropanoate

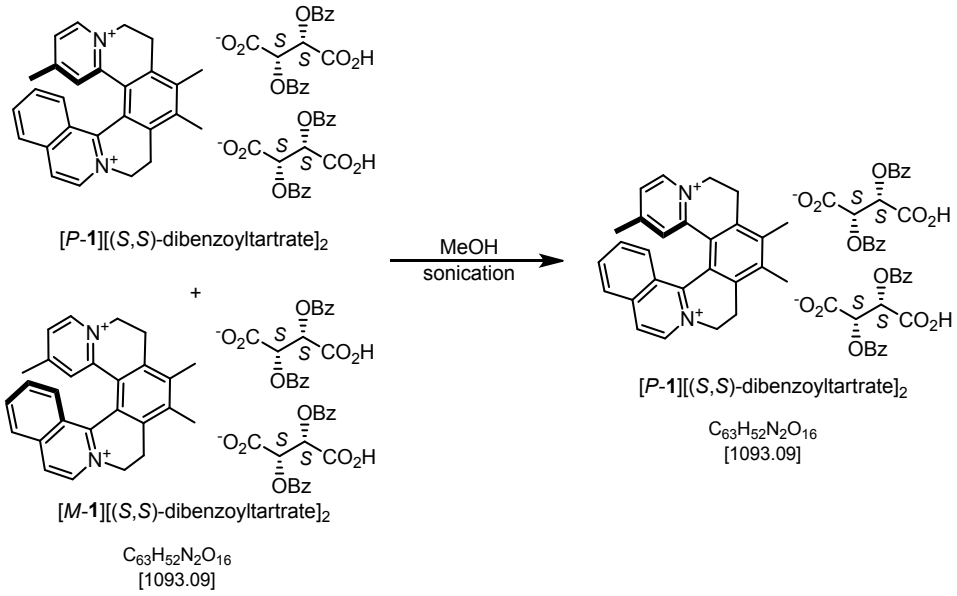

Mixture of diastereoisomeric salts [*P*-**1**][(*S*,*S*)-dibenzoyltartrate]$_2$ and [*M*-**1**][(*S*,*S*)-dibenzoyltartrate]$_2$ (923 mg) was suspended in MeOH (2 mL) and sonicated for 5 min. The resulting suspension was centrifuged and the supernatant was separated giving 432 mg of diastereomerically enriched mixture of salts ($[\alpha]_D$ = +264.0, c = 0.420, MeOH, 40 % *de* according to CE). The procedure of sonication, centrifugation and supernatant removal was repeated one more time with 2 mL and three more times with 1 mL of MeOH giving 242 mg of the [*P*-**1**][(*S*,*S*)-dibenzoyltartrate]$_2$ as an off-white solid (0.221 mmol, 52 % yield of (*P*,*S*,*S*)-diastereomer; $[\alpha]_D$ = +484.7, c = 0.262, MeOH; 98 % *de* according to CE). **Mp**: 149-151 °C; **^{1}H NMR** (600 MHz, DMSO-d$_6$): δ = 1.87 (s, 3H), 2.49 (s, 6H), 3.05-3.13 (m, 1H), 3.17-3.24 (m, 1H), 3.52-3.61 (m, 2H), 4.79 (td, *J* = 14.1, 3.4 Hz, 1H), 5.02-5.09 (m, 2H), 5.16-5.21 (m, 1H), 5.60 (s, 4H), 7.19 (d, *J* = 1.7 Hz, 1H), 7.42-7.47 (m, 8H), 7.54-7.61 (m, 6H), 7.83 (dd, *J* = 8.7, 0.8 Hz, 1H), 7.86-7.90 (m, 8H), 7.90-7.93 (m, 1H), 8.19 (d, *J* = 8.2 Hz, 1H), 8.52 (d, *J* = 6.6 Hz, 1H), 8.94 (d, *J* = 6.3 Hz, 1H), 9.05 (d, *J* = 6.7 Hz, 1H); **^{13}C NMR** (151 MHz, DMSO-d$_6$): δ = 16.5, 16.6, 20.4, 24.8, 25.2, 53.1, 54.4, 71.0, 122.2, 124.2, 125.2, 125.9, 126.5, 127.8, 128.6, 129.1, 129.3, 129.6, 131.2, 133.3, 135.0, 136.6, 137.6, 138.1, 139.5, 140.7, 141.0, 144.4, 145.3, 149.7, 157.2, 164.7, 167.6; **IR** (KBr): $\tilde{\nu}$ (cm^{-1}) 3066w, 1732vs, 1602m, 1585m, 1553w, 1510vw, 1493w, 1453s, 1319s, 1264vs, 1179m, 1160m, 711vs, 685m; **MS** (ESI) m/z: 735 (25, [M-DBT]$^+$), 377 (51, [M-2DBT-H]$^+$); **HRMS** (ESI) m/z: [M-DBT] ($C_{45}H_{39}O_8N_2$) calc. 735.27009, found 735.27046.

[*P*-1][TfO]$_2$

(*P*)-6,7,13-Trimethyl-4,5,8,9-tetrahydroisoquinolino[1,2-a]pyrido[1,2-k][2,9]phenanthroline-3,10-diium trifluoromethanesulfonate

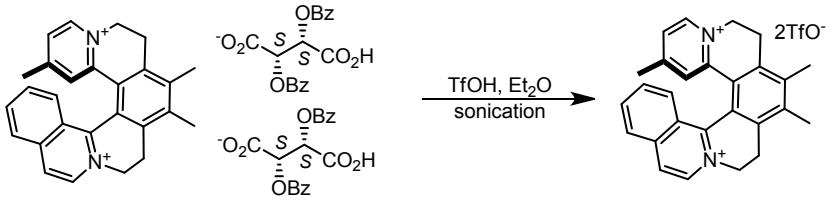

[*P*-**1**][(*S*,*S*)-dibenzoyltartrate]$_2$

$C_{63}H_{52}N_2O_{16}$
[1093.09]

[*P*-**1**][TfO]$_2$

$C_{29}H_{26}F_6N_2O_6S_2$
[676.65]

[*P*-**1**][(*S*,*S*)-dibenzoyltartrate]$_2$ (242 mg, 0.221 mmol) was suspended in triflic acid solution in Et_2O (TfOH : Et_2O = 1 : 99 volume ratio; 5 mL) and sonicated for 3 min. The resulting suspension was then centrifuged and the supernatant was separated. The procedure of sonication, centrifugation and supernatant separation was repeated two more times. To remove excess of triflic acid, diethylether (5 mL) was added, the mixture was sonicated, centrifuged and the supernatant was separated. The procedure of sonication, centrifugation and supernatant separation was repeated two more times. After drying, 142 mg of [*P*-**1**][TfO]$_2$ was isolated as an off-white solid (95 %, 0.210 mmol, $[\alpha]_D$ = +618.7, c = 0.245, MeOH; 98 % *ee* according to CE). The NMR spectra were identical to those of racemic sample [*rac*-**1**][TfO]$_2$,[2] see the NMR spectra section for the NMR scan.

[*M*-2][TfO]$_2$

(*M*)-(*E*)-13-(4-(dimethylamino)styryl)-6,7-dimethyl-4,5,8,9-tetrahydroisoquinolino[1,2-*a*]pyrido[1,2-*k*][2,9]phenanthroline-3,10-diium trifluoromethanesulfonate

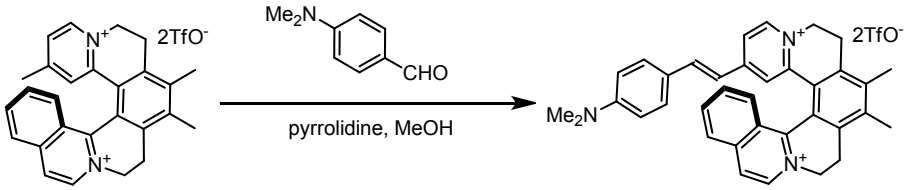

[*M*-**1**][TfO]$_2$

$C_{29}H_{26}F_6N_2O_6S_2$
[676.65]

[*M*-**2**][TfO]$_2$

$C_{38}H_{35}F_6N_3O_6S_2$
[807.82]

[*M*-**1**][TfO]$_2$ (11 mg, 0.0163 mmol) and 4-(dimethylamino)benzaldehyde (10 mg, 0.0670 mmol, 4 eq) were placed in a Schlenk flask and put under an argon atmosphere. MeOH (1 mL) was added and the solids were dissolved while stirring. The flask was covered with alufoil and pyrrolidine (17 µL, 14.5 mg, 0.2037 mmol, 12 eq) was added at once. The mixture was stirred at rt for 60 min, when the disappearance of the starting material was detected (by TLC, SiO_2, eluent: Stoddart's Magic mixture 7:2:1 MeOH:2M aq. solution of NH_4Cl:$MeNO_2$). The reaction was quenched with Et_2O (15 mL) causing precipitation. The suspension was centrifuged and the supernatant was separated. The residue was dissolved in MeOH (1 mL) by sonication and then the precipitation was effected by addition of Et_2O (15 mL). The suspension was centrifuged and the supernatant was separated. This dissolution-precipitation-centrifugation procedure was repeated once more using 1 mL MeOH and 15 mL Et_2O. The solids obtained after the last centrifugation and supernatant separation were dried under vacuum. This procedure gave 10 mg of product [*M*-**2**][TfO]$_2$ (0.0124 mmol, 76 %) as a dark violet solid. $[\alpha]_D$ =

-3063, c = 3.59 x 10^{-4} g/100mL, MeOH; 98 % *ee* according to CE. **Mp**: 264-266 °C (MeOH/Et_2O). $\mathbf{R_f}$ = 0.60 (SiO_2, eluent: Stoddart's Magic mixture 7:2:1 MeOH:2M aq. solution of NH_4Cl:$MeNO_2$); **^{1}H NMR** (600 MHz, acetone-d_6): δ = 2.57 (s, 3H), 2.58 (s, 3H), 3.07 (s, 6H), 3.27-3.35 (m, 1H), 3.37-3.45 (m, 1H), 3.70-3.77 (m, 2H), 5.09 (td, *J* = 13.9, 3.6 Hz, 1H), 5.14-5.22 (m, 2H), 5.32-5.37 (m, 1H), 6.54 (d, *J* = 16.0 Hz, 1H), 6.71 (d, *J* = 9.0 Hz, 2H), 7.14 (d, *J* = 16.0 Hz, 1H), 7.21 (d, *J* = 1.9 Hz, 1H), 7.39 (d, *J* = 8.9 Hz, 2H), 7.70 (dd, *J* = 1.9, 6.7 Hz, 1H), 7.73-7.76 (m, 1H), 7.91-7.94 (m, 1H), 8.08 (dd, *J* = 0.8, 8.8 Hz, 1H), 8.15 (d, *J* = 8.3 Hz, 1H), 8.52 (d, *J* = 6.7 Hz, 1H), 8.74 (d, *J* = 6.7 Hz, 1H), 9.05 (d, *J* = 6.7 Hz, 1H); **^{13}C NMR** (151 MHz, acetone-d_6): δ = 17.2, 17.3, 26.4, 26.7, 40.4, 54.2, 56.2, 113.0, 116.7, 120.6, 123.1, 123.4, 125.2, 125.6, 128.3, 128.9, 129.1, 131.4, 132.9, 136.6, 137.3, 138.8, 139.8, 141.2, 142.3, 142.8, 143.4, 144.9, 146.8, 151.8, 153.7, 154.7. **IR** (neat): $\tilde{\nu}$ (cm^{-1}) 1630w, 1571vs, 1547m, 1529m, 1509m, 1411w, 1369m, 1335m, 1255vs, 1224m, 1159s, 1110m, 1030s, 975w, br, 944w, 820w, 757vw, 637m, 573w, 517w; **MS** (ESI) m/z: 658 [$(M\text{-}TfO)^+$] (70), 508 [$(M\text{-}2TfO\text{-}H)^+$] (34), 254 [$M\text{-}2TfO\text{-}H)^{2+}$] (100); **HRMS** (ESI) m/z: [M-TfO] ($C_{37}H_{35}O_3N_3F_3S$) calc. 658.2346, found 658.2331.

[*P*-2][TfO]$_2$

(*P*)-(*E*)-13-(4-(dimethylamino)styryl)-6,7-dimethyl-4,5,8,9-tetrahydroisoquinolino[1,2-*a*]pyrido[1,2-*k*][2,9]phenanthroline-3,10-diium trifluoromethanesulfonate

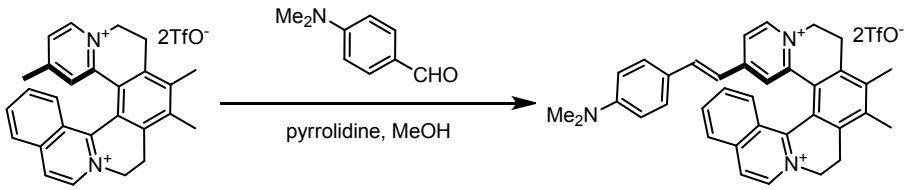

[*P*-**1**][TfO]$_2$ $C_{29}H_{26}F_6N_2O_6S_2$ [676.65]

[*P*-**2**][TfO]$_2$ $C_{38}H_{35}F_6N_3O_6S_2$ [807.82]

[*P*-**1**][TfO]$_2$ (11 mg, 0.0163 mmol) and 4-(dimethylamino)benzaldehyde (10 mg, 0.0670 mmol, 4 eq) were placed in a Schlenk flask and put under an argon atmosphere. MeOH (1 mL) was added and the solids were dissolved while stirring. The flask was covered with alufoil and pyrrolidine (16 µL, 13.6 mg, 0.1917 mmol, 12 eq) was added in a single portion. The mixture was stirred at rt for 60 min, when the disappearance of the of the starting material was detected (by TLC, SiO_2, eluent: Stoddart's Magic mixture 7:2:1 MeOH:2M aq. solution of NH_4Cl:$MeNO_2$). The reaction was quenched with Et_2O (15 mL) causing precipitation. The suspension was centrifuged and the supernatant was separated. The residue was dissolved in MeOH (1 mL) by sonication and then the precipitation was effected by addition of Et_2O (15 mL). The suspension was centrifuged and the supernatant was separated. This dissolution-precipitation-centrifugation procedure was repeated once more using 1 mL MeOH and 15 mL Et_2O. The solids obtained after the last centrifugation and supernatant separation were dried under vacuum. This procedure gave 7 mg of product [*P*-**2**][TfO]$_2$ (0.0087 mmol, 53 %) as a dark violet solid. $[\alpha]_D$ = +3223, c = 3.71 x 10^{-4} g/100mL, MeOH; 98 % *ee* according to CE. **Mp**: 259-261 °C (MeOH/Et_2O); $\mathbf{R_f}$ = 0.60 (SiO_2, eluent: Stoddart's Magic Mixture 7:2:1 MeOH:2M aq. solution of NH_4Cl:$MeNO_2$); **^{1}H NMR** (600 MHz, acetone-d_6): δ = 2.57 (s, 3H), 2.58 (s, 3H), 3.07 (s, 6H), 3.27-3.35 (m, 1H), 3.37-3.45 (m, 1H), 3.69-3.76 (m, 2H), 5.05-5.12 (m, 1H), 5.13-5.22 (m, 2H), 5.32-5.37 (m, 1H), 6.54 (d, *J* = 16.0 Hz, 1H), 6.71 (d, *J* = 9.0 Hz, 2H), 7.14 (d, *J* = 16.0 Hz, 1H), 7.21 (d, *J* = 1.9 Hz, 1H), 7.39 (d, *J* = 8.9 Hz, 2H), 7.69 (dd, *J* = 2.0, 6.7 Hz, 1H), 7.72-7.76 (m, 1H), 7.90-7.93 (m, 1H), 8.07 (dd, *J* = 0.8, 8.7 Hz, 1H), 8.15 (d, *J* = 8.2 Hz, 1H), 8.51 (d, *J* = 6.7 Hz, 1H), 8.73 (d, *J* = 6.7 Hz, 1H), 9.04 (d, *J* = 6.7 Hz, 1H); **^{13}C NMR** (151 MHz, acetone-d_6): δ = 16.9, 16.9, 26.4, 26.7, 40.1, 54.0,

56.3, 112.6, 117.0, 119.9, 123.4, 123.5, 125.2, 126.0, 126.8, 128.3, 128.9, 128.9, 131.4, 132.5, 136.1, 137.8, 138.6, 139.7, 140.7, 142.2, 142.2, 143.2, 144.8, 146.7, 151.9, 153.3, 154.7; **IR** (neat): $\tilde{\nu}$ (cm^{-1}) 1631w, 1572vs, 1547m, 1529m, 1509m, 1411w, 1370m, 1336m, 1258vs, 1224m, 1161s, 1111m, 1030s, 975w, br, 944w, 819w, 757vw, 637m, 574w, 517w; **MS** (ESI) m/z: 658 (70, $[M\text{-}TfO]^+$), 508 (34, $[M\text{-}2TfO\text{-}H]^+$), 254 (100, $[M\text{-}2TfO\text{-}H)]^{2+}$); **HRMS** (ESI) m/z: [M-TfO] ($C_{37}H_{35}O_3N_3F_3S$) calc. 658.2346, found 658.2331.

Chiral Purity

Chiral analysis was performed by capillary electrophoresis (CE) with sulfated cyclodextrin-based chiral selector.[10,12-14] The Beckman-Coulter MDQ apparatus with a photodiode array (PDA) modul was used. Analytes were detected by UV absorption at 200 nm. Capillaries were Polymicro fused silica TSP050375 (Polymicro Technologies, Phoenix, AZ, USA) of 50/370 mm id/od. The capillaries were coated with hydroxypropylcellulose (HPC) as described in [15,16] and used for experiments in 29.5/39.5 cm effective/total length. A background electrolyte consisted of 22 mM sodium + 35 mM phosphate buffer, pH 2.4, and a chiral selector, which was 12 mM heptakis(2,3-di-O-acetyl-6-O-sulfo)-β-cyclodextrin[17] (Sigma Aldrich, cat. no. 28205). Solid helquat samples **1** and **2** were dissolved in water and methanol, respectively, and injected as approx. 0.5 mM solutions into the capillary by pressure of 1.4 kPa for 5 s. Separation voltage was –12 kV (i.e. cathode at the injection capillary end), capillary temperature was 22 °C and generated current was 40 μA. See Figs. S11 and S12 for the CE charts.

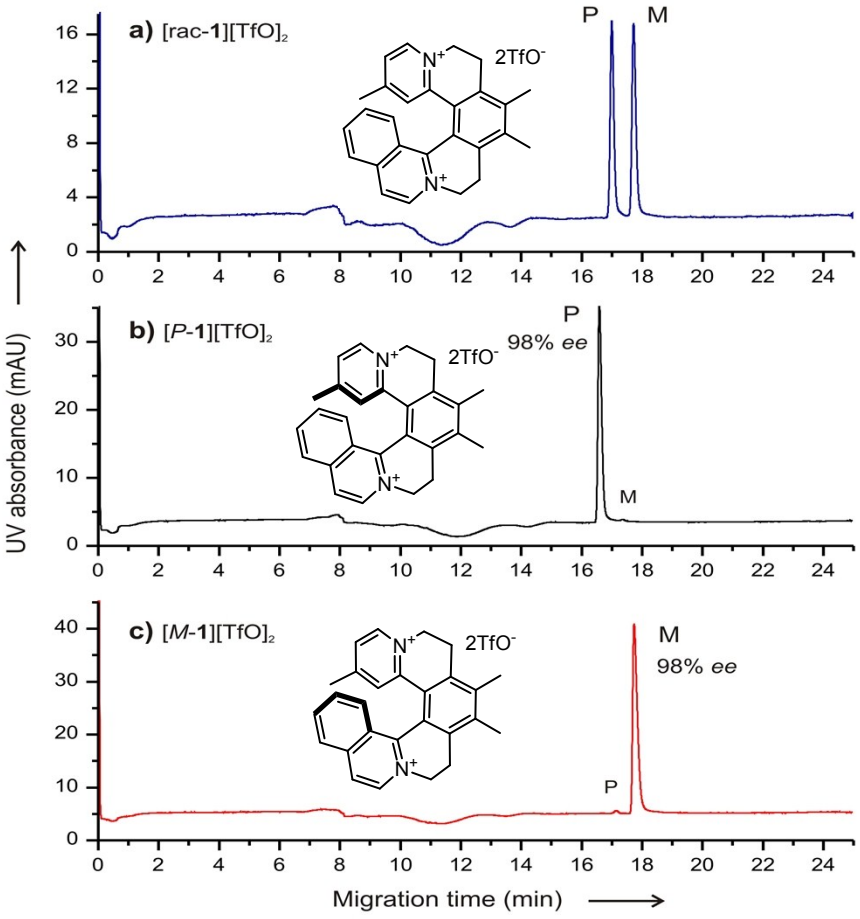

Fig. S11 Chiral analysis of helquat **1** (i.e. dye precursor) samples using capillary electrophoresis with chiral selector. a) [*rac*-**1**][TfO]$_2$, b) [*P*-**1**][TfO]$_2$ and c) [*M*-**1**][TfO]$_2$. See the text above for experimental details.

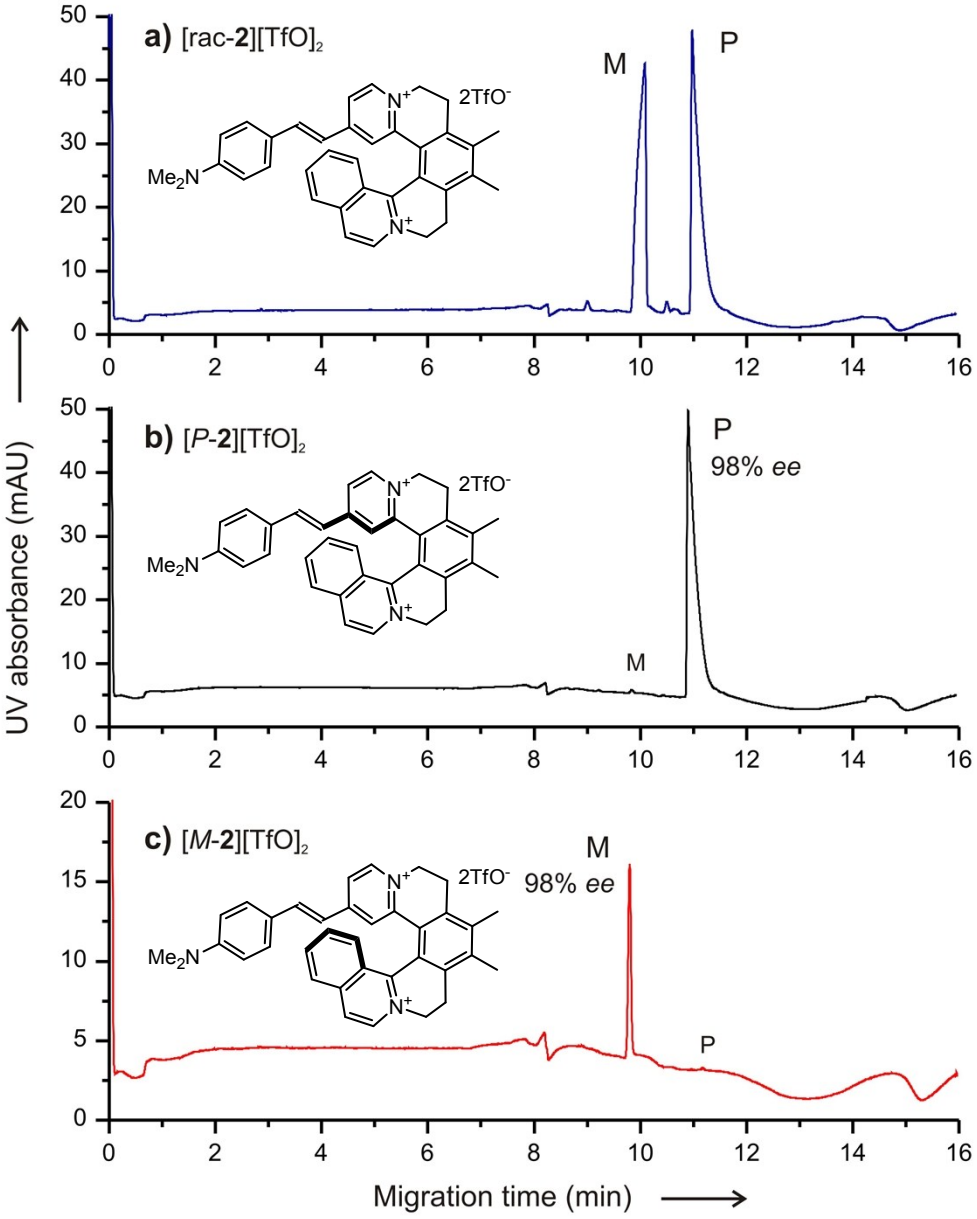

Fig. S12 Chiral analysis of helquat dye **2** samples using capillary electrophoresis with chiral selector. a) [*rac*-**2**][TfO]$_2$, b) [*P*-**2**][TfO]$_2$ and c) [*M*-**2**][TfO]$_2$. See the text above for experimental details.

X-ray analysis

Crystallographic data for **[*M*-1][TfO]$_2$ (CCDC 925832)** and **[*P*-1][I]$_2$ (CCDC 925833)** were collected on Nonius KappaCCD diffractometer equipped with Bruker APEX-II CCD detector by monochromatized MoKα radiation (λ = 0.71073 Å) at a temperature of 150(2) K. The determination of absolute configuration of corresponding derivatives were based on anomalous dispersion of sulfur or iodine atoms.

The structures were solved by direct methods (SHELXS)[18] and refined by full matrix least squares based on F^2 (SHELXL97).[18] The absorption corrections were carried on using multi-scan method. The hydrogen atoms were found on difference Fourier map and were recalculated into idealized positions. All hydrogen atoms were refined as fixed (riding model) with assigned temperature factors $H_{iso}(H)$ = 1.2 U_{eq}(pivot atom) or 1.5 U_{eq} for methyl moiety.

[*M*-1][TfO]$_2$ (CCDC 925832):

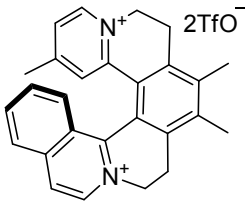

[*M*-**1**][TfO]$_2$

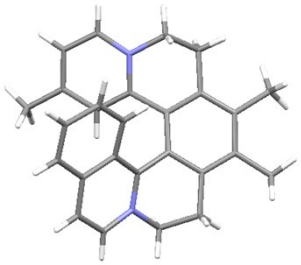

In the crystal structure above the anions and solvent molecules were omitted for clarity. The determination of absolute configuration of [*M*-**1**][TfO]$_2$ was based on anomalous dispersion of sulfur atoms.

Preparation of X-ray quality crystals of the [*M*-1][TfO]$_2$

***Crystallization**:* X-ray quality crystals were grown *via* slow diffusion of *i*-Pr_2O into a acetonitrile/methanol solution of the [*M*-**1**][TfO]$_2$ (*ca* 3 days, fridge, 7 °C). Counter anions and molecules of solvent were omitted for clarity.

Crystal data for [*M*-**1**][TfO]$_2$ (CCDC 925832): $2(C_{27}H_{26}N_2)\bullet4(CF_3O_3S)\bullet C_2H_3N$, M_r = 1394.33; Monoclinic, $P2_1$ (No 4), a = 11.6454 (7) Å, b = 12.5993 (6) Å, c = 21.7275 (14) Å, β = 104.608 (2)° , V = 3084.9 (3) Å^3, Z = 2, D_x = 1.501 Mg m^{-3}, colorless plate of dimensions 0.55 × 0.27 × 0.11 mm, multi-scan absorption correction (μ = = 0.26 mm^{-1}), T_{min} = 0.873, T_{max} = 0.972; a total of 47506 measured reflections (θ_{max}= 27.5˚), from which 14180 were unique (R_{int} = 0.023) and 12241 observed according to the $I > 2\sigma(I)$ criterion. The refinement converged (Δ/σ_{max}= 0.002) to R = 0.040 for observed reflections and w$R(F^2)$ = 0.110, *GOF* = 1.02 for 845 parameters and all 14180 reflections. The final difference Fourier map displayed no peaks of chemical significance ($\Delta\rho_{max}$ = 0.47, $\Delta\rho_{min}$ = -0.29 e.Å^{-3}). Chirality parameter (Flack) −0.05 (4).

[*P*-1][I]$_2$ (CCDC 925833):

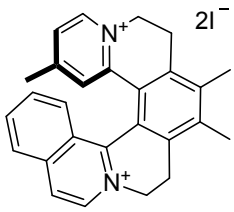

[*P*-**1**[I]$_2$

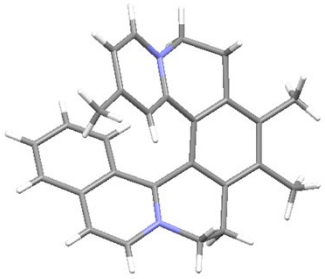

In the crystal structure above the anions and solvent molecules were omitted for clarity. The determination of absolute configuration of [*P*-**1**][I]$_2$ was based on anomalous dispersion of iodine atoms.

Preparation of X-ray quality crystals of the [*P*-1][I]$_2$ starting from [*P*-1][TfO]$_2$

Ion exchange*:* [*P*-**1**][TfO]$_2$ (15 mg, 0.022 mmol, 1 eq) was dissolved in minimum amount of acetone (approximately 0.5 mL). NaI (17mg, 0.11 mmol, 5 eq) was dissolved in minimum amount of acetone (approximately 0.5 mL). Solutions were mixed and yellow precipitate appeared. The suspension was centrifuged and the solids were separated from the supernatant. The solids were then sonicated with acetone (0.5 mL). The suspension was again centrifuged and the solids were dried *in vacuo*. [*P*-**1**][I]$_2$ was obtained in 56 % yield (8 mg, 0.013 mmol) as a pale-yellow solid.

Crystallization*:* X-ray quality crystals were grown *via* slow diffusion of *i*-Pr$_2$O into a nitromethane solution of the [*P*-**1**][I]$_2$ (*ca* 7 days, fridge, 7 °C).

Crystal data for [*P*-**1**][I]$_2$ (CCDC 925833): $C_{27}H_{26}N_2$•CH_3NO_2•2(I), M_r = 693.34; Orthorhombic, $P2_12_12_1$ (No 19), a = 7.9386 (2) Å, b = 17.6476 (4) Å, c = 19.6814 (4) Å, V = 2757.31 (11) Å^3, Z = 4 D_x = 1.670 g m^{-3}, red plate of dimensions 0.51 × 0.20 × 0.08 mm, numerical absorption correction (μ = 2.31 mm^{-1}), T_{min} = 0.385, T_{max} = 0.840; a total of 40066 measured reflections (θ_{max}= 27.5˚), from which 6334 were unique (R_{int} = 0.021) and 6087 observed according to the $I > 2\sigma(I)$ criterion. The refinement converged (Δ/σ_{max}= 0.009) to R = 0.018 for observed reflections and w$R(F^2)$ = 0.043, *GOF* = 1.04 for 320 parameters and all 6334 reflections. The final difference Fourier map displayed no peaks of chemical significance ($\Delta\rho_{max}$ = 0.73, $\Delta\rho_{min}$ = -0.41 e.Å^{-3}). Chirality parameter (Flack) -0.031 (12).

Crystallographic data have been deposited with CCDC no. 925832 and 925833 for [*M*-**1**][TfO]$_2$ and [*P*-**1**][I]$_2$, respectively and can be obtained free of charge from Cambridge Crystallographic Data Centre *via* https: //summary.ccdc.cam.ac.uk/structure-summary-form

Preparation of liquid HCN was adapted according to procedure published by Pézolet and Savoie instead of cooling with liquid nitrogen the trap with dry ice-aceton was used.[19] *Warning the HCN is extremely poisonous gas or liquid penetrating through skin*.

References

[1] J. Šebestík, P. Bouř, *J. Phys. Chem. Lett.,* **2011**, *2*, 498-502.

[2] D.A. Case, T.A. Darden, T.E. Cheatham, III, C.L. Simmerling, J. Wang, R.E. Duke, R. Luo, M. Crowley, R.C. Walker, W. Zhang, K.M. Merz, B. Wang, S. Hayik, A. Roitberg, G. Seabra, I. Kolossváry, K.F. Wong, F. Paesani, J. Vanicek, X. Wu, S.R. Brozell, T. Steinbrecher, H. Gohlke, L. Yang, C. Tan, J. Mongan, V. Hornak, G. Cui, D.H. Mathews, M.G. Seetin, C. Sagui, V. Babin, and P.A. Kollman (2008), AMBER 10, University of California, San Francisco.

[3] L. Martínez, R. Andrade, E. G. Birgin, J. M. Martínez. Packmol: A package for building initial configurations for molecular dynamics simulations. *J. Comput. Chem.* **2009**, *30*, 2157-2164.

[4] E.F. Pettersen, T.D. Goddard, C.C. Huang, G.S. Couch, D.M. Greenblatt, E.C. Meng, T.E. Ferrin, *J. Comput. Chem.* **2004**, *25*, 1605-1612.

[5] P. Bouř, J. Sopková, L. Bednarová, P. Maloň, T.A. Keiderling, *J. Comput. Chem.* **1997**, *18*, 646-659.

[6] T. Yanai, D. Tew, N. Handy, *Chem. Phys. Lett.* **2004**, *393,* 51-57.

[7] a) A. D. Becke, *Phys. Rev. A* **1988**, *38,* 3098-3100. b) J. P. Perdew, in *Electronic Structure of Solids '91*, Ed. P. Ziesche and H. Eschrig (Akademie Verlag, Berlin, 1991) 11. c) . P. Perdew, J. A. Chevary, S. H. Vosko, K. A. Jackson, M. R. Pederson, D. J. Singh, C. Fiolhais, *Phys. Rev. B* **1992**, *46*, 6671-6687. d) J. P. Perdew, J. A. Chevary, S. H. Vosko, K. A. Jackson, M. R. Pederson, D. J. Singh, C. Fiolhais, *Phys. Rev. B* **1993**, *48*, 4978. e) J. P. Perdew, K. Burke, Y. Wang, *Phys. Rev. B*, **1996**, *54,* 16533-16539. f) K. Burke, J. P. Perdew, and Y. Wang, in *Electronic Density Functional Theory: Recent Progress and New Directions*, Ed. J. F. Dobson, G. Vignale, and M. P. Das (Plenum, 1998).

[8] S. Yamamoto, P. Bouř, *J. Comput. Chem.* **2013**, *34*, 2152-2158.

[9] D. B. Amabilino, P. R. Ashton, A. S. Reder, N. Spencer, J. F. Stoddart, *Angew. Chem. Int. Ed. Engl.* **1994**, *33*, 1286-1290; *Angew. Chem.* **1994**, *106*, 1316-1319.

[10] P. E. Reyes-Gutiérrez, M. Jirásek, L. Severa, P. Novotná, D. Koval, P. Sázelová, J. Vávra, A. Meyer, I. Císařová, D. Šaman, R. Pohl, P. Štěpánek, P. Slavíček, B. J. Coe, M. Hájek, V. Kašička, M. Urbanová, F. Teplý, *Chem. Commun.* **2015**, *51*, 1583-1586.

[11] J. Vávra, L. Severa, P. Švec, I. Císařová, D. Koval, P. Sázelová, V. Kašička, F. Teplý, *Eur. J. Org. Chem.* **2012**, 489-499.

[12] D. Koval, L. Severa, L. Adriaenssens, J. Vávra, F. Teplý, V. Kašička, *Electrophoresis* **2011**, *32*, 2683-2692.

[13] L. Adriaenssens, L. Severa, D. Koval, I. Císařová, M. Martínez Belmonte, E. C. Escudero-Adán, P. Novotná, P. Sázelová, J. Vávra, R. Pohl, D. Šaman, M. Urbanová, V. Kašička, F. Teplý, *Chem. Sci.* **2011**, *2*, 2314-2320.

[14] L. Severa, M. Ončák, D. Koval, R. Pohl, D. Šaman, I. Císařová, P. E. Reyes-Gutiérrez, P. Sázelová, V. Kašička, F. Teplý, P. Slavíček, *Angew. Chem. Int. Ed.* **2012**, *51*, 11972-11976; *Angew. Chem.* **2012**, *124*, 12138–12142.

[15] Y. F. Shen, R. D. Smith, *J. Micro. Sep.* **2000**, *12*, 135-141.

[16] D. Koval, V. Kašička, H. Cottet, *Anal. Biochem.* **2011**, *413*, 8-15.

[17] J. B. Vincent, A. D.Sokolowski, T. V. Nguyen, G. Vigh, *Anal. Chem.* **1997**, *69*, 4226-4233.

[18] G. M. Sheldrick, *Acta Cryst.* A64, **2008**, 112-122.

[19] M. Pézolet, R. Savoie, *Canad. J. Chem.*, **1969**, *47*, 3041-3048.

NMR spectra

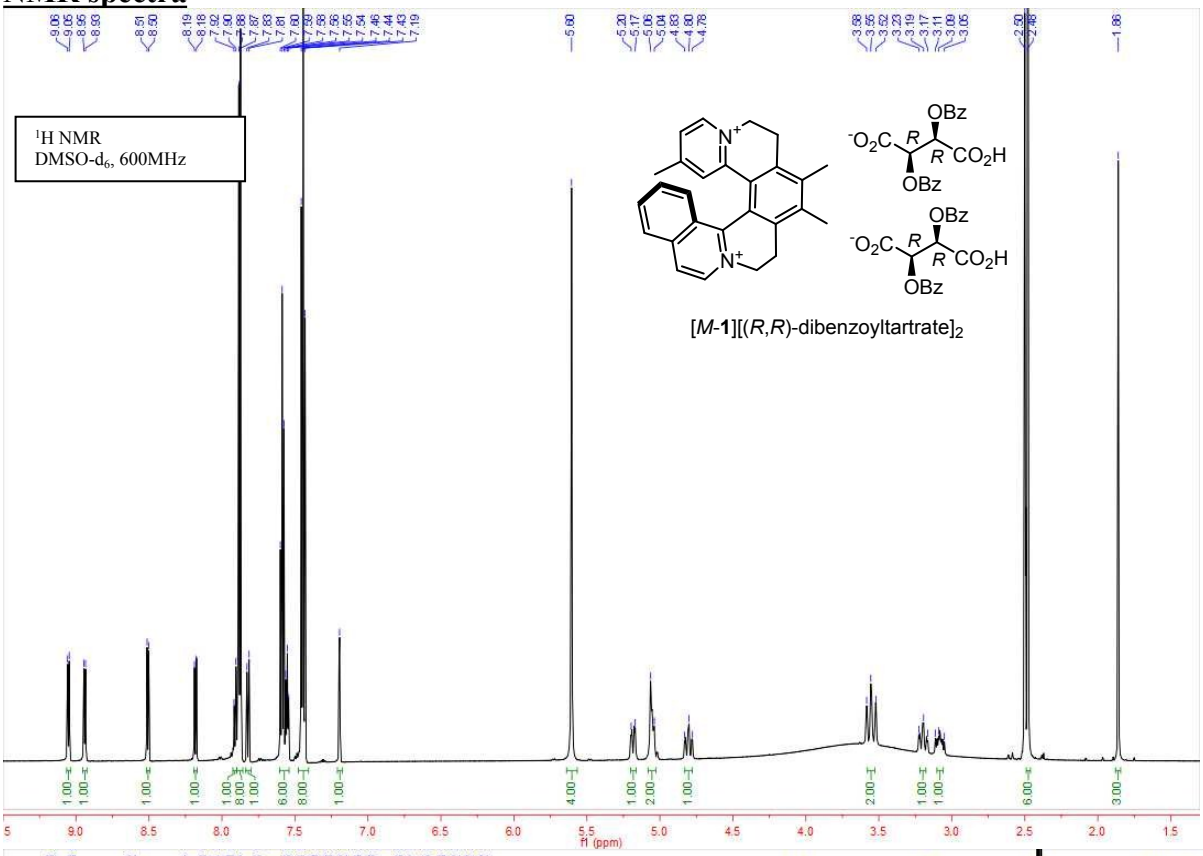
^{1}H NMR
DMSO-d$_6$, 600MHz
[*M*-**1**][(*R*,*R*)-dibenzoyltartrate]$_2$

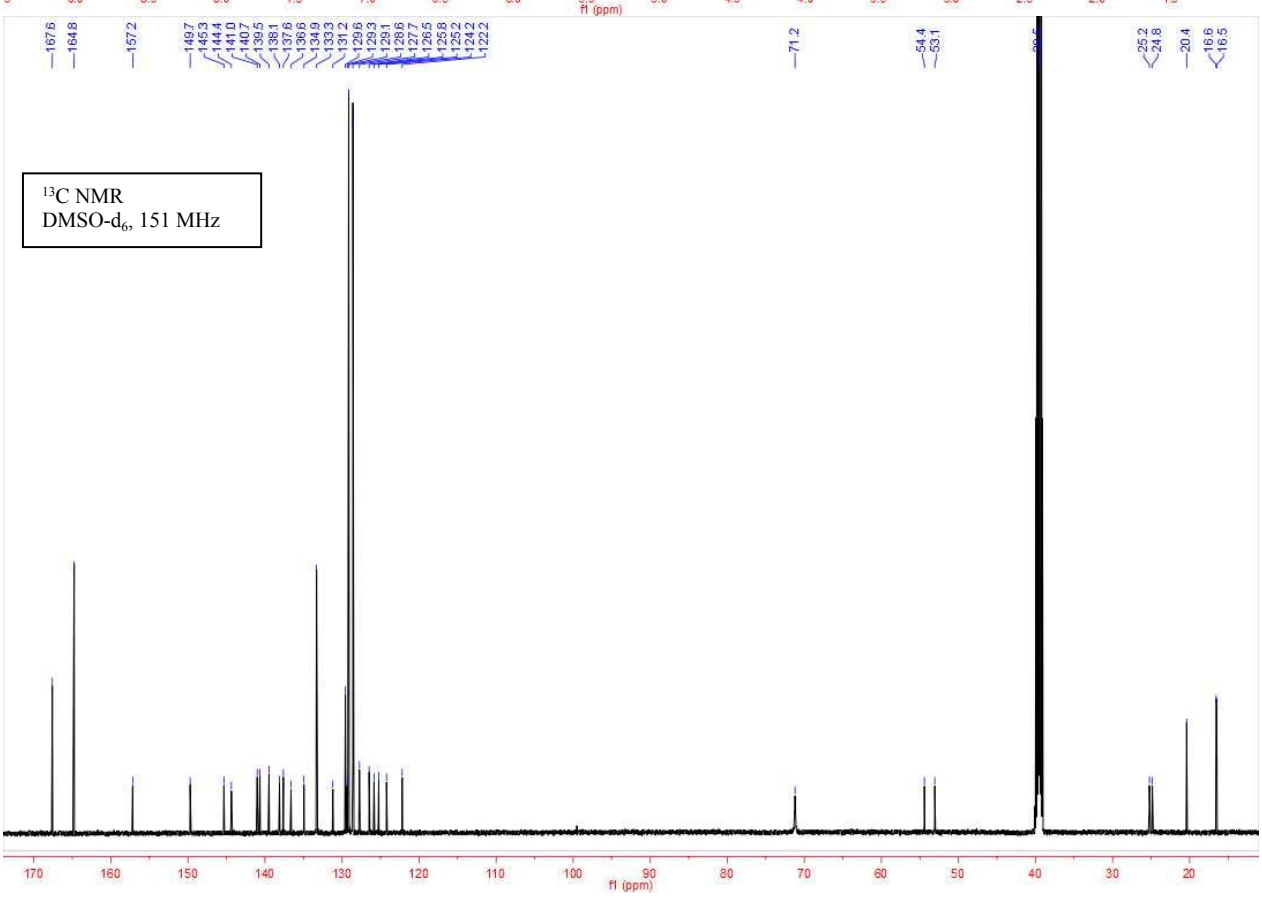
^{13}C NMR
DMSO-d$_6$, 151 MHz

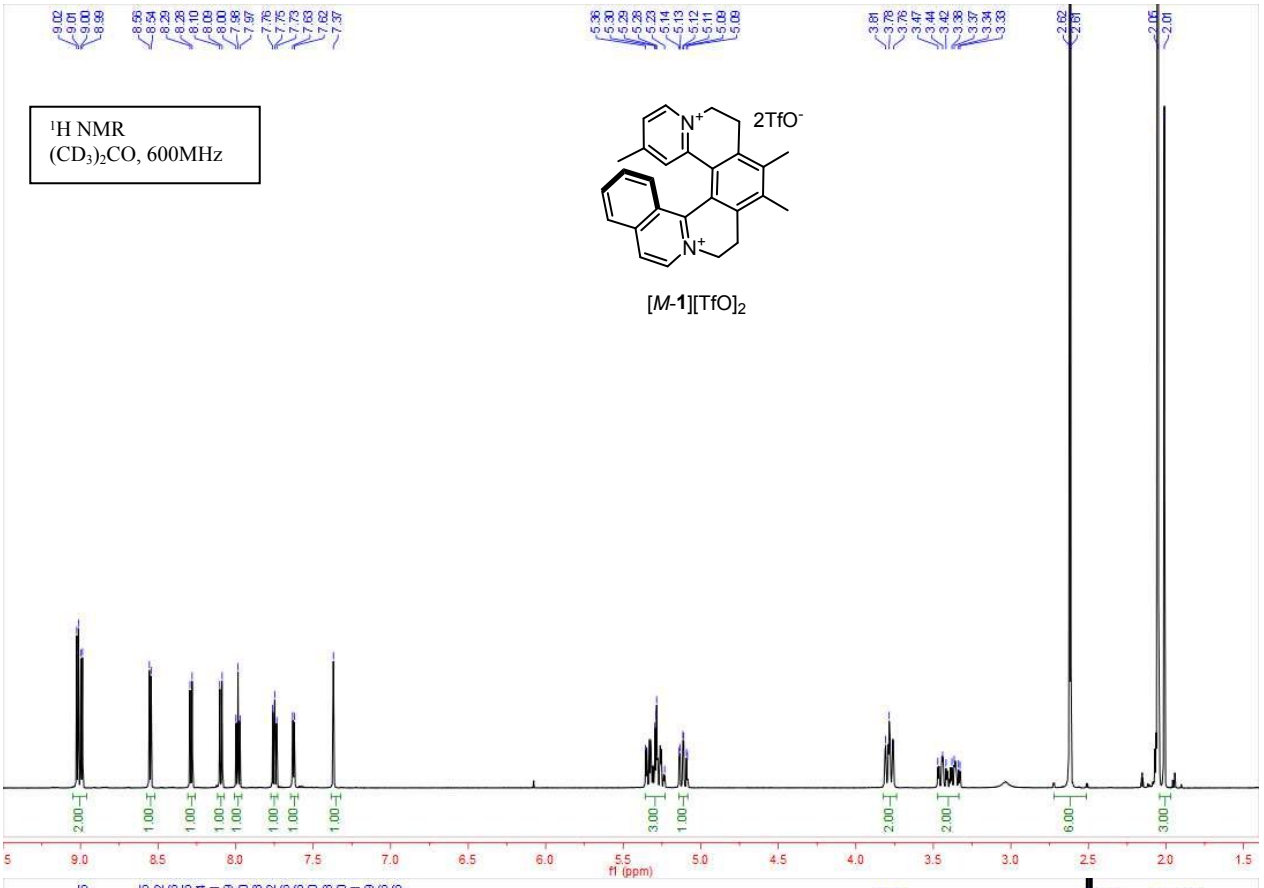
[1]H NMR
(CD3)2CO, 600MHz
2TfO-
[M-1][TfO]2
f1 (ppm)

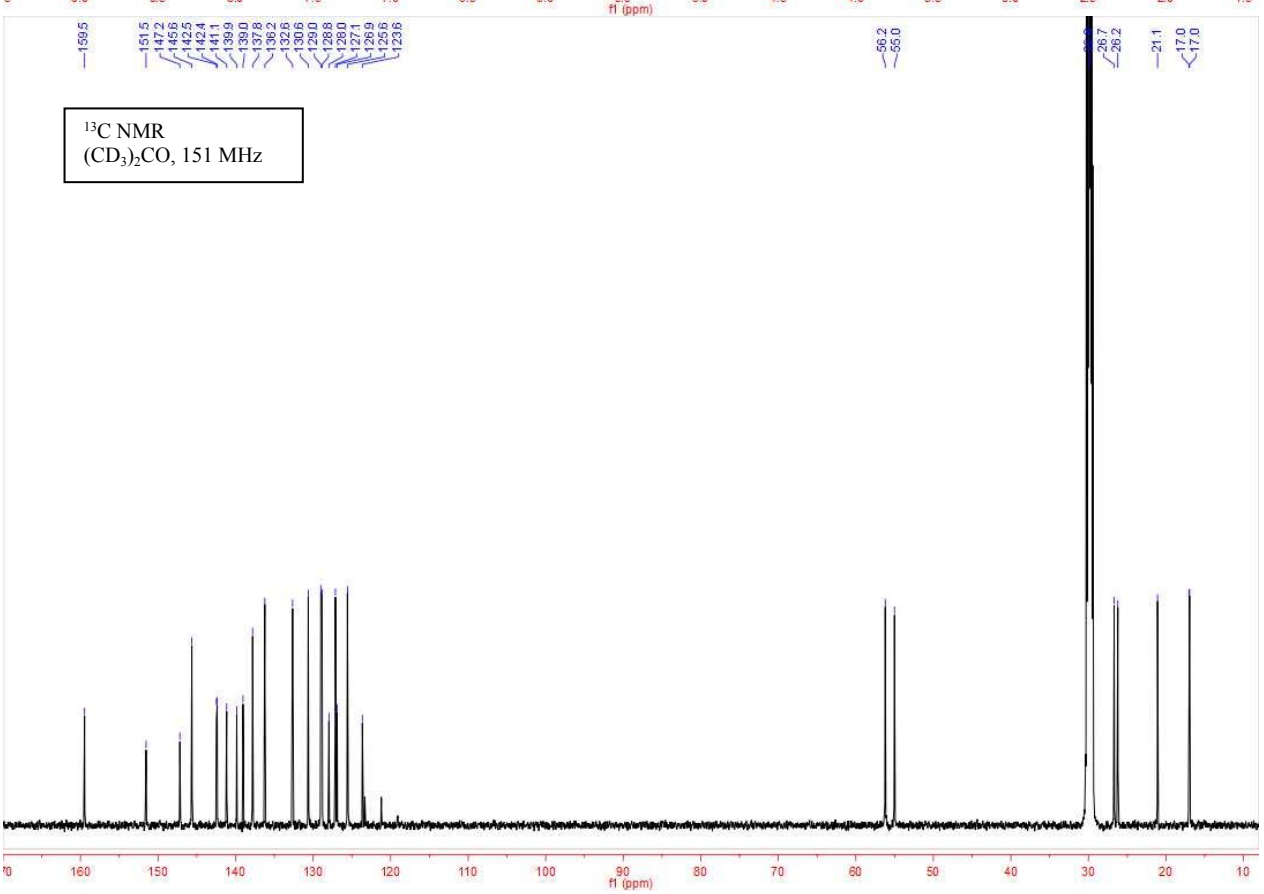
[13]C NMR
(CD3)2CO, 151 MHz
f1 (ppm)

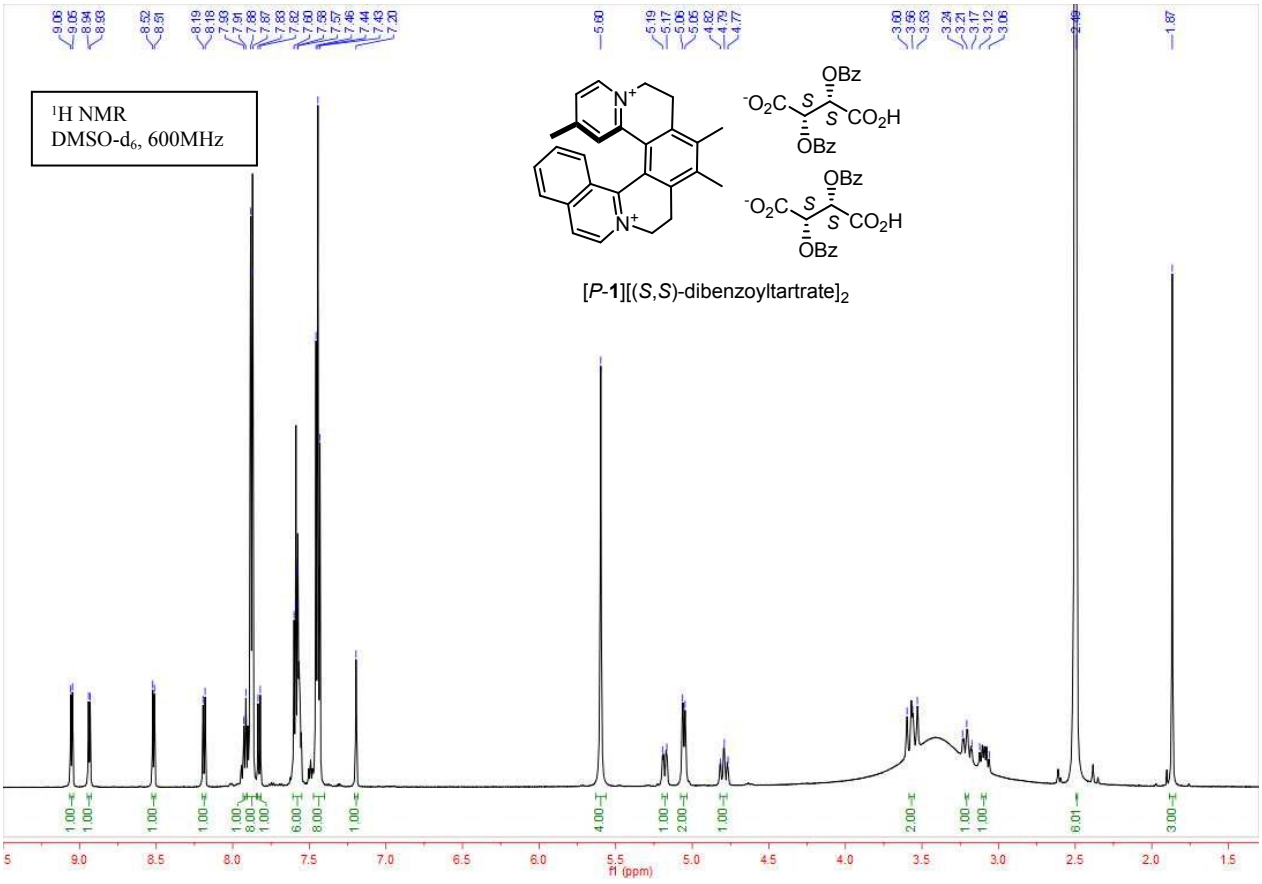
^{1}H NMR
DMSO-d$_6$, 600MHz
[*P*-**1**][(*S*,*S*)-dibenzoyltartrate]$_2$
f1 (ppm)

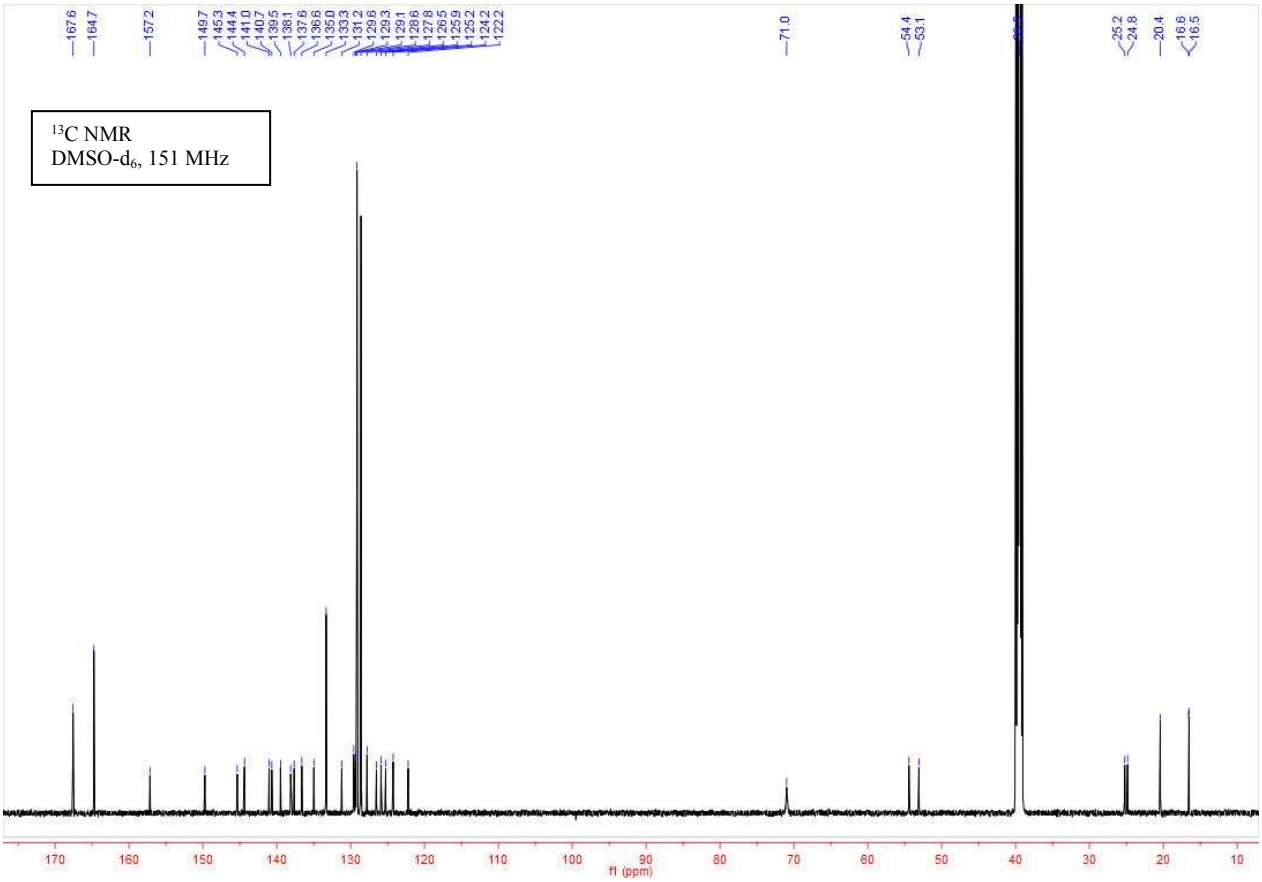
^{13}C NMR
DMSO-d$_6$, 151 MHz
f1 (ppm)

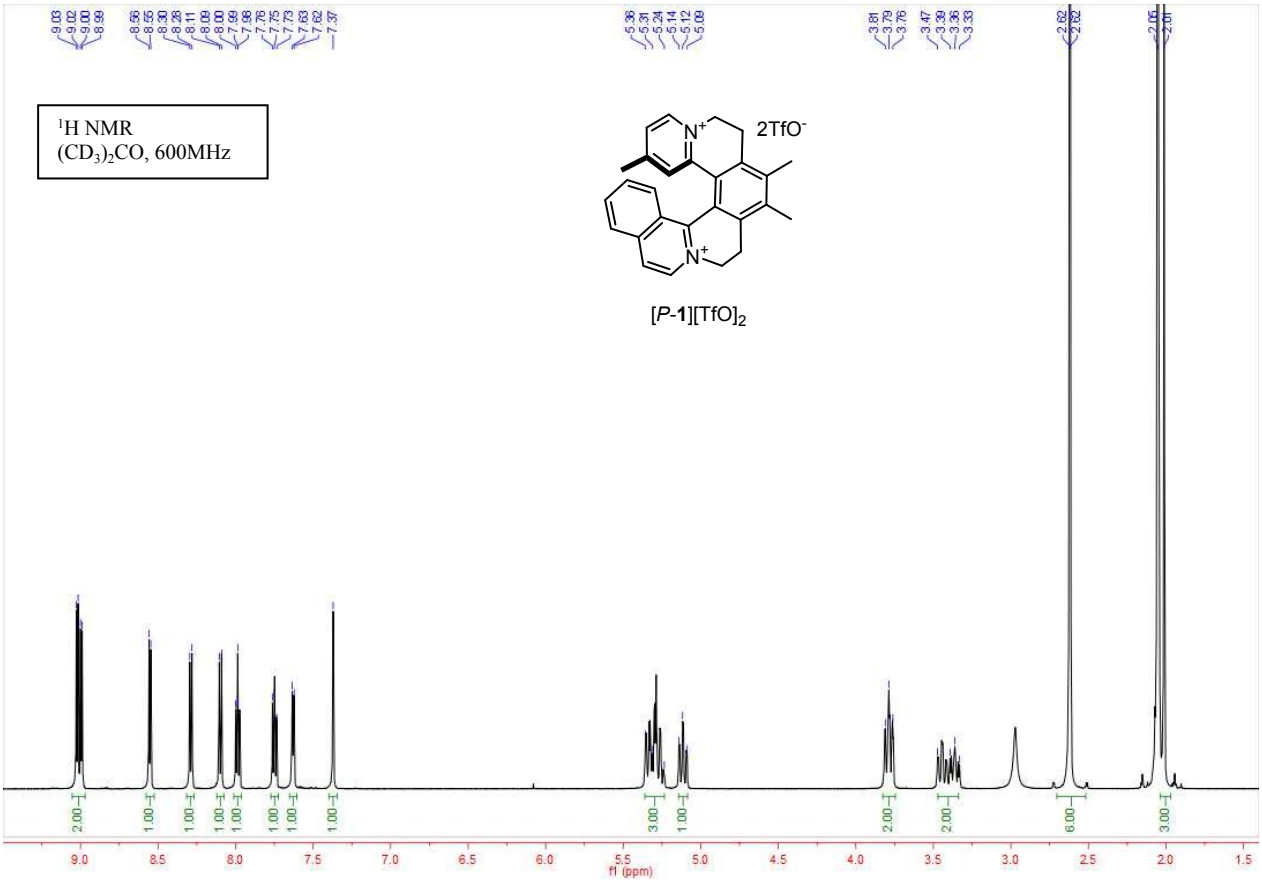
^{1}H NMR
$(CD_3)_2CO$, 600MHz
2TfO$^-$
[*P*-**1**][TfO]$_2$
f1 (ppm)

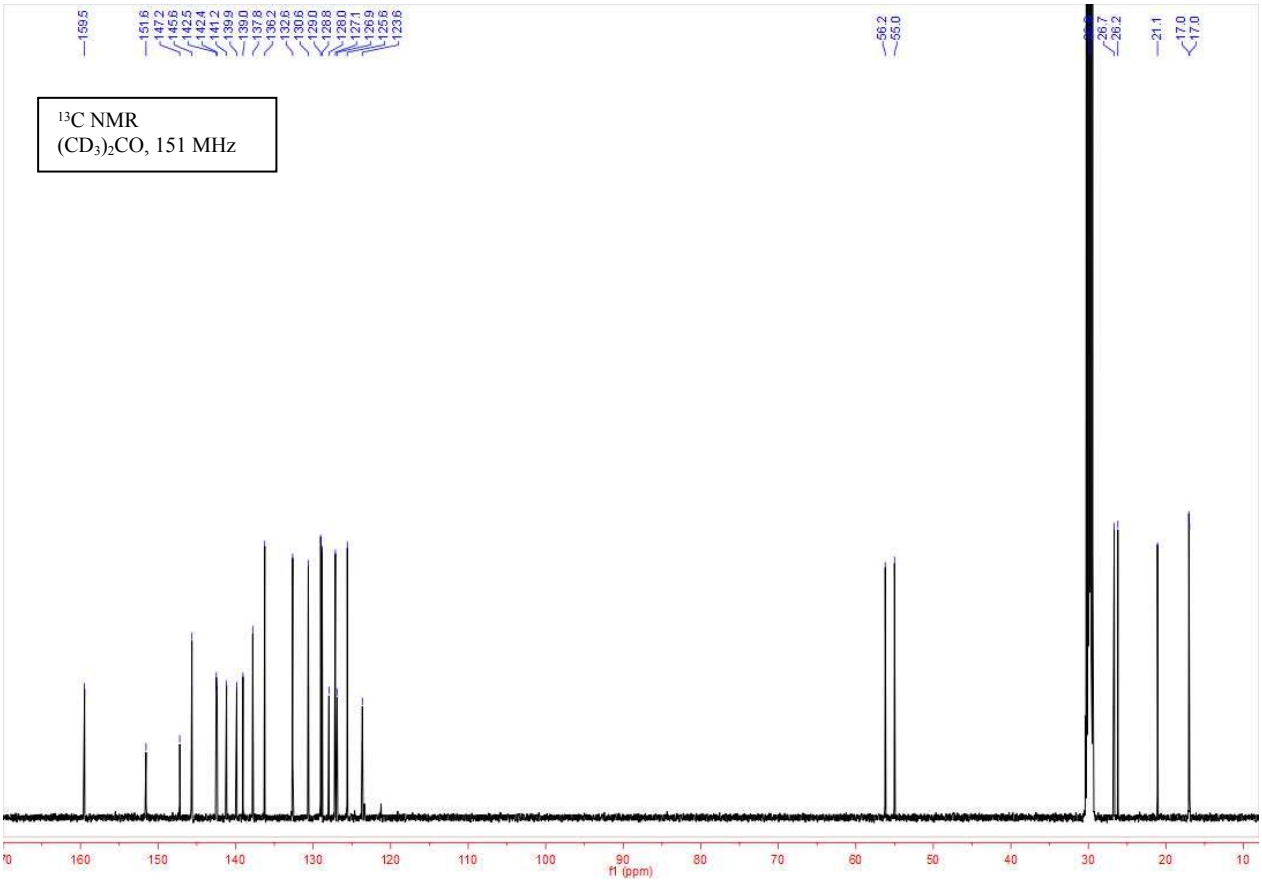
^{13}C NMR
$(CD_3)_2CO$, 151 MHz
f1 (ppm)

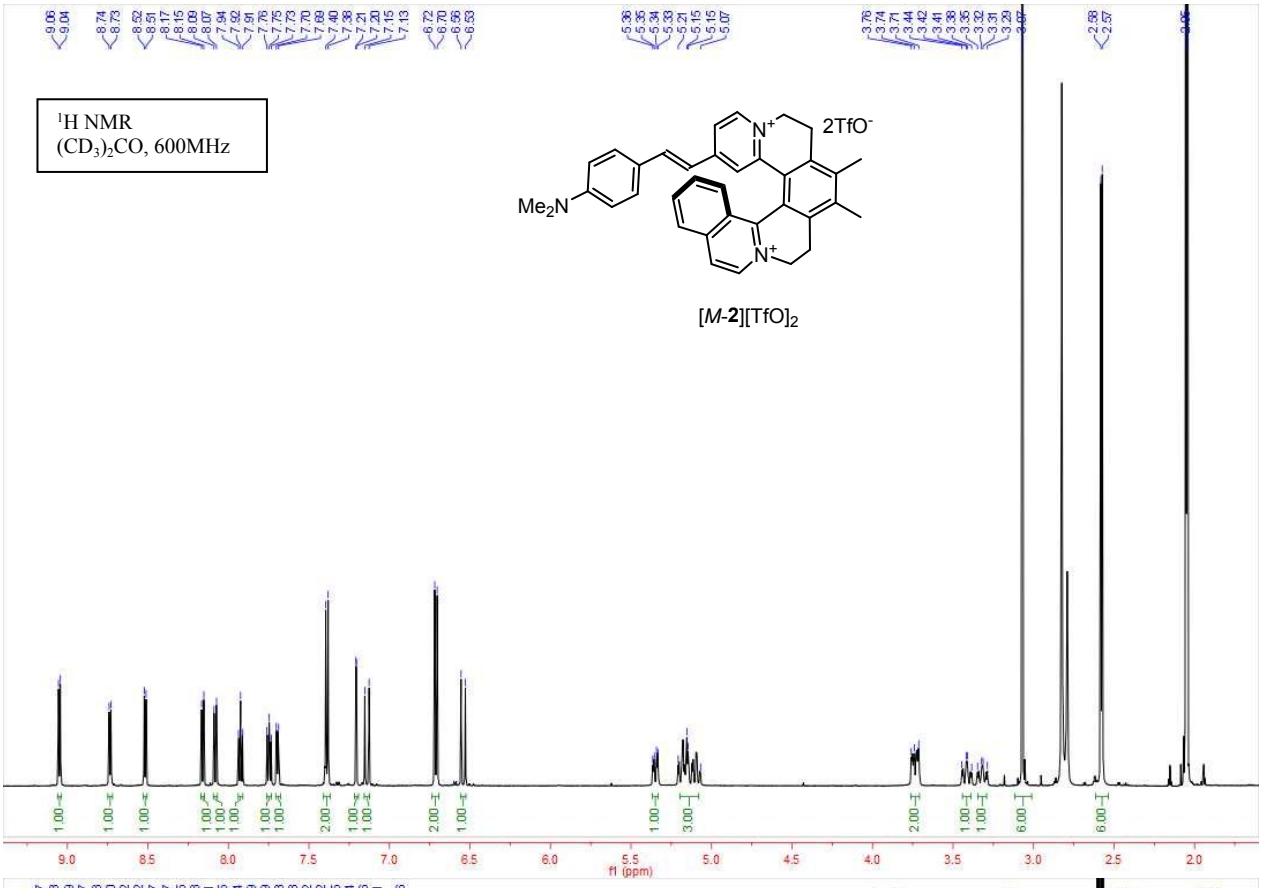
^{1}H NMR
$(CD_3)_2CO$, 600MHz
Me_2N
N^+
$2TfO^-$
N^+
[*M*-**2**][TfO]$_2$
f1 (ppm)

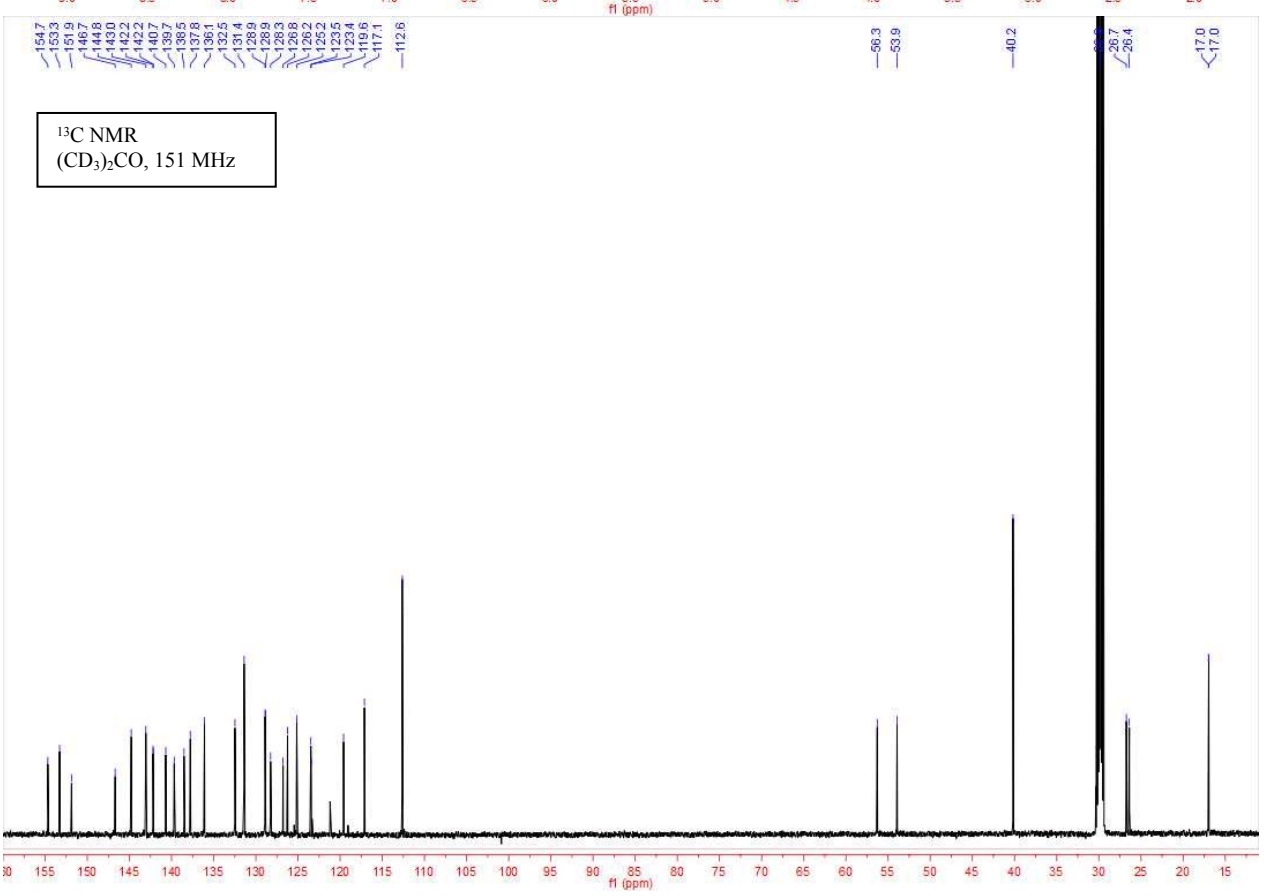
^{13}C NMR
$(CD_3)_2CO$, 151 MHz
f1 (ppm)

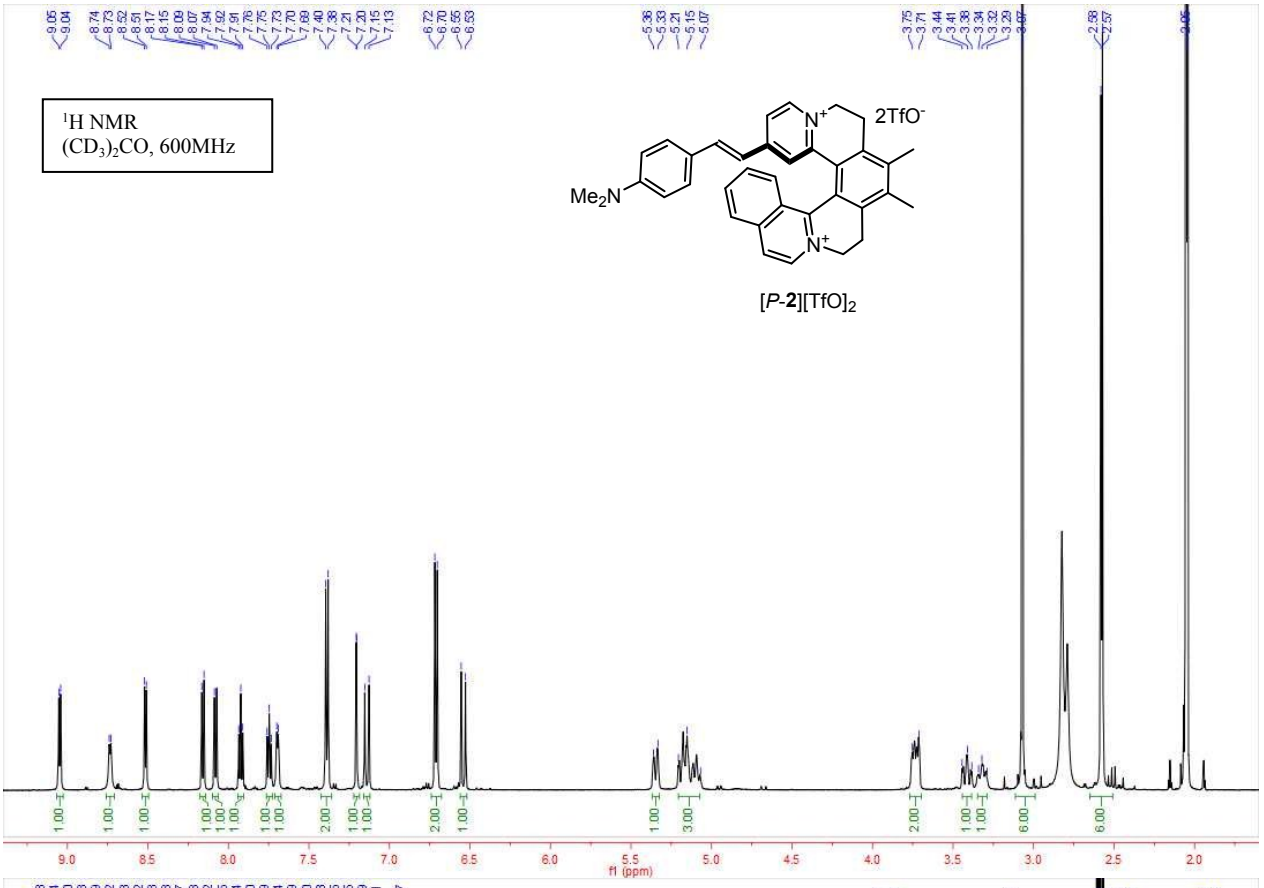

^{1}H NMR
$(CD_3)_2CO$, 600MHz

[*P*-**2**][TfO]$_2$

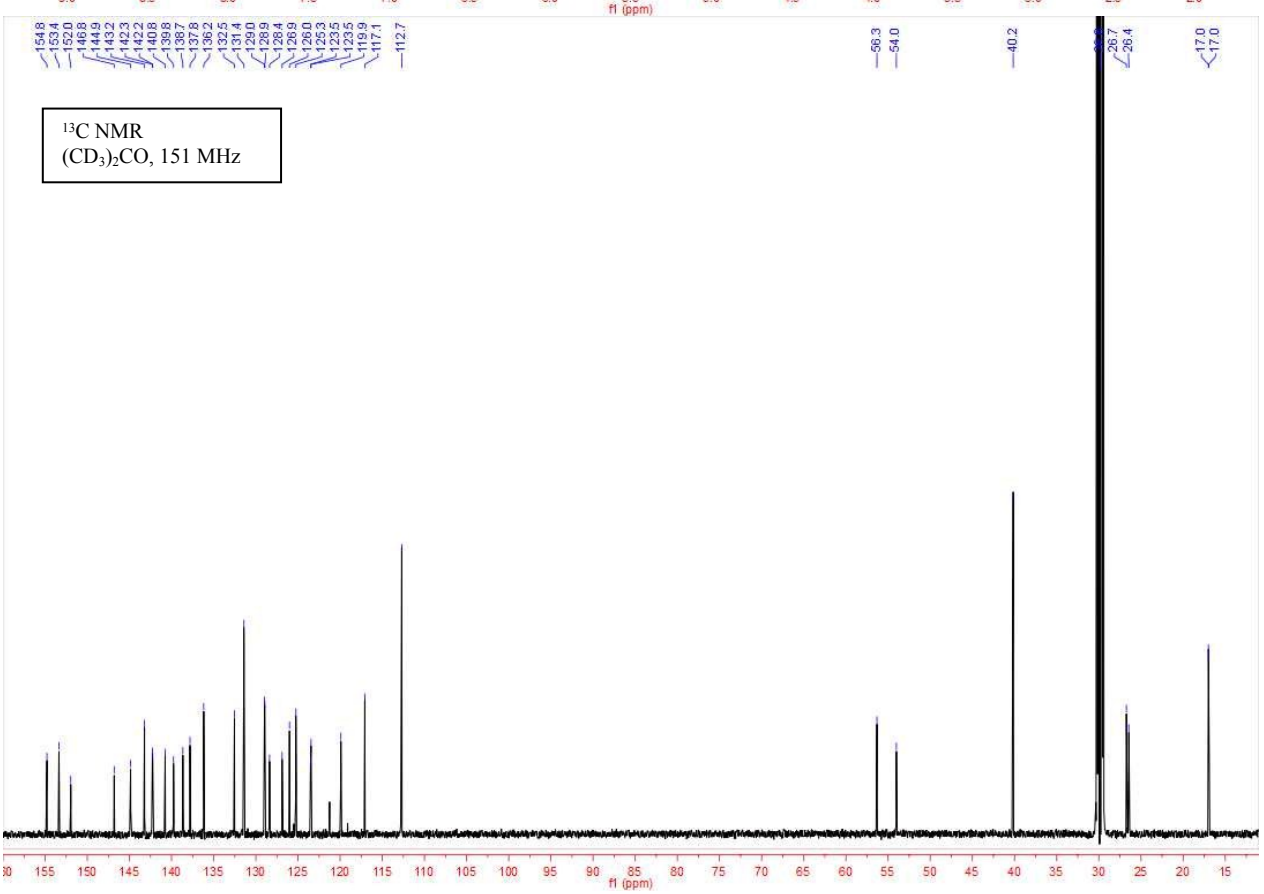

^{13}C NMR
$(CD_3)_2CO$, 151 MHz